

Rowan University

Rowan Digital Works

Theses and Dissertations

6-13-2017

Effects of passive and active training paradigms on bone and muscle recovery after spinal cord injury

Brittany Lynn King
Rowan University

Follow this and additional works at: <https://rdw.rowan.edu/etd>



Part of the [Biomedical Engineering and Bioengineering Commons](#), and the [Mechanical Engineering Commons](#)

Recommended Citation

King, Brittany Lynn, "Effects of passive and active training paradigms on bone and muscle recovery after spinal cord injury" (2017). *Theses and Dissertations*. 2440.
<https://rdw.rowan.edu/etd/2440>

This Thesis is brought to you for free and open access by Rowan Digital Works. It has been accepted for inclusion in Theses and Dissertations by an authorized administrator of Rowan Digital Works. For more information, please contact graduateresearch@rowan.edu.

**EFFECTS OF PASSIVE AND ACTIVE TRAINING PARADIGMS ON BONE
AND MUSCLE RECOVERY AFTER SPINAL CORD INJURY**

by

Brittany L. King

A Thesis

Submitted to the
Department of Mechanical Engineering
College of Engineering
In partial fulfillment of the requirement
For the degree of
Master of Science in Mechanical Engineering
at
Rowan University
May 5th, 2017

Thesis Chair: Dr. Jennifer Kadlowec

Acknowledgments

First and foremost, I would like to thank my advisor throughout the entire project, Dr. Singh, whom not only acted as my advisor, but as a wonderful mentor and teacher throughout both my undergraduate and graduate years. I am able to finish this project with invaluable knowledge and experience all thanks to the time and work that Dr. Singh put forth in allowing this project to come to fruition. I would also like to thank my thesis committee members, Dr. Kadlowec and Dr. Beachley, for their time and guidance.

I want to also thank my fellow Rowan University students, alumni, and staff for their participation in this project to design and build the treadmills used. I would like to thank the Rowan School of Osteopathic Medicine staff for the space to work in complete our project. I want to thank the students, especially Sarah Townsend, at Widener University who helped with the data collection and analysis throughout the project, and the Tech Park CT Scanning Room at Rowan University for its X-Ray and Micro-CT equipment. For their craftsmanship in building the bikes, I would like to thank the staff at Drexel University. Lastly, I would like to thank the New Jersey Commission on Spinal Cord Exploratory Research for supporting our grant, #CSCR14ERG001.

Lastly, to my parents: I want to thank you for all of your love and support throughout not only this project, but my entire journey up to this point—it is because of your constant motivation and belief in me that I was able to overcome the hardships and doubts in my mind and achieve my dreams and aspirations. I appreciate your patience, understanding, and help over the years, and hope you know how meaningful you both are to me. Thank you.

Abstract

Brittany King

EFFECTS OF PASSIVE AND ACTIVE TRAINING PARADIGMS ON BONE RECOVERY AFTER SPINAL CORD INJURY IN ANIMALS

2016-2017

Dr. Jennifer Kadlowec

Master of Science in Mechanical Engineering

The effects spinal cord injury (SCI) has have been studied in both human and animal models. Specifically in incomplete SCI, the bone degradation and muscle atrophy seen in the lower limbs has been documented, along with the effects of different training paradigms on bone and muscle loss. This study implemented a clinically relevant animal model of a moderate spinal contusion injury at the T9—T10 level, along with active body weight supported treadmill training (BWSTT) and passive bike training, to compare the effects such training methods have on the bone microstructure properties and muscle masses in the lower limbs of rats. Behavioral BBB and wire grid testing, along with three-point bending, was conducted. Our results showed that both passive and active trained animals did not show any significant differences from normal animals in metaphyseal region bone volume over total volume (BV/TV), and bike trained animals had no significant differences in trabecular separation (Tb.Sp) from normal animals. Further comparisons were drawn from the remaining properties of trabecular thickness (Tb.Th), trabecular number (Tb.N), and soleus muscle masses. This study allows for a comprehensive view of bone recovery on SCI with active and passive training paradigms.

Table of Contents

Abstract.....	iv
List of Figures.....	ix
List of Tables.....	xiv
Chapter 1: Introduction.....	1
1.1 Problem Statement.....	2
1.2 Hypothesis.....	2
Chapter 2: Human Bone and Spine.....	4
2.1 Bone Anatomy.....	4
2.2 Microstructural Anatomy.....	5
2.2.1 Cortical Bone.....	6
2.2.2 Trabecular Bone.....	7
2.2.3 Bone Growth and Resorption.....	7
2.2.4 Tibia Anatomy.....	10
2.3 The Spine.....	11
2.3.1 The Vertebral Column.....	11
2.3.2 The Spinal Cord.....	18
2.3.3 Spinal Cord Injury.....	20
Chapter 3: Bone and Muscle Changes Following Spinal Cord Injury.....	26
3.1 Introduction.....	26
3.2 Muscle Atrophy Morphology.....	26

Table of Contents (Continued)

3.3 Bone Loss Morphology.....	28
3.4 Human Studies.....	29
3.4.1 Muscle Changes.....	29
3.4.2 Bone Changes.....	30
3.4.3 Testing Techniques.....	33
3.5 Animal Studies.....	37
3.5.1 Muscle Changes.....	37
3.5.2 Bone Changes.....	38
3.5.3 Testing Techniques.....	38
3.6 Conclusion.....	40
Chapter 4: Current Rehabilitation Strategies to Restore Bone Loss after Spinal Cord Injury.....	
4.1 Introduction.....	41
4.2 Passive Training.....	41
4.3 Active Training.....	44
4.4 Human Studies.....	45
4.4.1 Passive Training.....	45
4.4.2 Active Training.....	46
4.5 Animal Studies.....	47
4.5.1 Passive Training.....	47

Table of Contents (Continued)

4.5.2 Active Training.....	49
4.6 Goal.....	50
Chapter 5: Effects of Training Paradigms on Bone Recovery after Spinal Cord	
Injury in Animals.....	52
5.1 Abstract.....	52
5.2 Introduction.....	53
5.2.1 Current Aim.....	54
5.3 Methods & Materials.....	54
5.3.1 Spinal Cord Injury.....	54
5.3.2 Animal Care.....	56
5.3.3 Behavioral Analysis.....	56
5.3.4 Treadmill Training.....	57
5.3.5 Bike Training.....	59
5.3.6 Animal Sacrifice.....	59
5.3.7 Bone Analysis.....	60
5.3.8 Muscle Mass.....	63
5.4 Results.....	63
5.4.1 Behavioral Analysis.....	63
5.4.2 Bone Analysis.....	64
5.4.3 Three-Point Bending.....	67

Table of Contents (Continued)

5.4.4 Muscle Mass.....	68
5.5 Discussion.....	69
5.6 Conclusion.....	73
Chapter 6: Future Work.....	75
6.1 Introduction.....	75
6.2 Alternative Training Methods and Paradigms.....	76
6.2.1 Functional Electrical Stimulation (FES) Training.....	76
6.2.2 Combination Training Paradigms.....	79
6.3 Histology.....	82
6.3.1 Spinal Cord Histology.....	82
6.3.2 Bone Histology.....	85
6.3.3 Muscle Histology.....	86
6.4 Conclusion.....	87
References.....	88

List of Figures

Figure	Page
Figure 1. Human skeleton with examples of the four bone types [73].....	4
Figure 2. Diagram of a femur bone, with the diaphysis and metaphysis marked [6].....	5
Figure 3. Diagram of metaphysis region with outer cortical and inner trabecular bone [7].....	6
Figure 4. Diagram of four remodeling stages, with phase 1 activation, phase 2 resorption, phase 3 reversal and phase 4 formation [6].....	9
Figure 5. Anatomy of the tibia [11].....	11
Figure 6. The five regions of the vertebral column [14].....	12
Figure 7. Superior and Lateral views of the lumbar vertebra, made up of the vertebral body and arch [14].....	13
Figure 8. Different views of the vertebral discs and their anatomical components and functions to load [14].....	14
Figure 9. Lateral view comparison of (A) rat and (B) human spinal column from the C2—L2 levels [15].....	17
Figure 10. Diagram of cross section of the spinal cord and its protective layers [14]...	18
Figure 11. Diagram of the 31 segments of the spinal cord [14].....	20

Figure 12. ASIA grading scales for neurological impairment (boxed, center) and muscle function (top left) along with incomplete vs. complete classification (right) [18].....	22
Figure 13. Drawing of a healthy, normal muscle and a muscle undergoing atrophy....	27
Figure 14. Bone density scan of a normal bone, and one that is osteoporotic and incurred bone loss. [42].....	28
Figure 15. MicroCT image for calculating trabecular thickness (A) and separation (B) 3D distances computed by fitting spheres inside background. [39].....	32
Figure 16. Comparison of axis for different planes (coronal, top and transverse, bottom) in calculating the number of trabecula in tibia bone [40].....	33
Figure 17. Diagram of standard three-point bending set-up. Bone is placed between two bottom points and top, force applied point [41].....	34
Figure 18. Variables measured from three-Point bending tests conducted on normal (S.I.) and osteoporotic (OSP) trabecular bone [80].....	36
Figure 19. Biomechanical testing via three-point bending on SCI rats two, four and six weeks post injury versus the noninjured control group [45].....	39
Figure 20. Example of passive training device meant to stretch the radiocarpal (wrist) joint [49].....	42
Figure 21. Example of passive training device meant to stretch hip, knee, and ankle joints [50].....	43

Figure 22. Schematic of body weight supported treadmill for active training [4].....	44
Figure 23. Passive cycling set-up with FES of hind limb training [53].....	46
Figure 24. Scanned electron microscopy (SEM) images of the femur and tibia of normal rats, SCI rats, SCI with passive standing (PS) rats, and SCI with electrical stimulation (ES) rats after 63 days [8].....	48
Figure 25. Wire Grid behavioral analysis set up.....	57
Figure 26. Images of the custom built body weight support treadmill. (A) National Instruments myDAQ system, paired with LabVIEW VI operating system;....	58
Figure 27. Trainer with rat, demonstrating BWSTT.....	58
Figure 28. Image of bike set up. (A) Rectangular frame for holding rat, screwed into place by adjustable knobs attached to vertical metal rods;	59
Figure 29. Rat tibia in para-film wrapped tube on top of metal brass stage prepared for scanning.....	60
Figure 30. Longitudinal image of rat tibia metaphysis (top) and diaphysis (bottom) regions scanned.....	61
Figure 31. Three-point bending device set up.....	62
Figure 32. Graph of baseline and weekly BBB scores for rat groups.....	63

Figure 33. Graph of wire grid testing of differences in normal stepping to missteps in uninjured animals, and injury only, BWSTT, and Bike groups 8 weeks post-SCI.....	64
Figure 34. (a) Percentage to normal rats of diaphyseal and metaphyseal BV/TV in SCI rats;	65
Figure 35. 3D Reconstruction of trabecular bone from (a) normal; (b) injury; (c) BWSTT and (d) Bike rats.....	67
Figure 36. Three-point bending results for normal, injury, BWSTT and Bike rats for average loads until bending.....	68
Figure 37. Soleus muscle mass as its percentage to total rat body weight for normal, injury, BWSTT and Bike rats.....	69
Figure 38. A patient standing with FES placed on her knee, hip, trunk extensors, and hip and trunk abductors and adductors [59].....	78
Figure 39. A patient walking with an 8 channel [59].....	79
Figure 40. A patient on an ergometer, with electrodes attached to his lower limbs [64].....	80
Figure 41. A paraplegic walking with FES and BWSTT with leg-gait assistance [66].....	81
Figure 42. Histology slide of the spinal [69]	83

Figure. 43. LFB staining of SCI and control (sham) groups comparing white matter from 24h—10weeks post injury [68]..... 85

List of Tables

Table	Page
Table 1. Description of the numerous SCI animal models used in spinal research to simulate human SCI [24]	25
Table 2. Number of Animals in each group.....	55

Chapter 1

Introduction

As of 2016, spinal cord injury (SCI) is found in about 54 people per million individuals in the United States, with an additional 17,000 cases approximated to be added every year. The most common causes of SCI are vehicular accidents, making up about 38% of all injury causes, with falls, acts of violence, and sports related injuries rounding out the top four most common reasons. Both complete and incomplete injuries can be found in either tetraplegia or paraplegia. Incomplete tetraplegia is the most common neurological diagnosis, making up about 45% of all SCI cases. This refers to an ‘incomplete’ SCI, such that there are spared pathways, but the injury affects both the upper and lower halves of the body, compared to paraplegia which just affects the lower half. [1].

Even after one gets through the initial injury, there are numerous changes that occur in the body following the weeks and months post-injury. Atrophy and degradation of the muscles and bones of the paralyzed joints is dependent upon the severity of the SCI, caused from the immobility and inability for the person to use their limbs and generate and support any mechanical force [2]. Due to the occurrence of SCI, along with the detrimental effects the injury can have on the body, therapeutic techniques and training paradigms have been studied and utilized to try and reduce the degradation, as well as regain some of the density and biomechanical properties in the bones and muscles. Two commonly seen training methods include passive training, seen in cycling,

and active training, seen in body weight supported treadmill training (BWSTT), both providing their own set of advantages [3,4].

Many animal studies have been conducted allowing for a more in depth assessment of the effects training can have on bone and muscle recovery following SCI that cannot be as easily done in humans. Passive standing, cycling, and treadmill training were amongst past therapies employed, with bone biomechanical properties as well as muscle masses compared to training versus injured only and control groups. To grasp a better understanding of what training paradigms may actually be more advantageous for SCI persons, conducting a study that entails both passive and active training techniques will be beneficial.

1.1 Problem Statement

This study aims to assess the changes in bone and muscle recovery following rehabilitation paradigms of both active body weight supported treadmill training (BWSTT) and passive cycling training in a clinically relevant thoracic (T9—10) level contusion spinal cord injury (SCI) animal model.

1.2 Hypothesis

Our hypothesis for this study is that: (1) Body weight supported treadmill training and bike training following spinal cord injury will cause differences in bone microarchitectural properties while overall reducing the amount of bone degradation and muscle atrophy in hind limbs compared to non-trained, spinal cord injured groups; and (2) Active body weight supported treadmill training will have more of an effect in

reducing bone degeneration and muscle atrophy that passive bike training following spinal cord injury.

Chapter 2

Human Bone and Spine

2.1 Bone Anatomy

The human skeleton, as an adult, contains 213 bones, excluding the sesamoid bones. Of these bones, four unique categories can be distinguished which are: long bones, short bones, flat bones, and irregular bones (Fig. 1). The first includes bones such as the ulnae, humeri, fibulae, femurs and tibiae, the latter two being a main focus in this study to record their structural changes following spinal cord injury (SCI). The second type includes the sesamoid bones, patellae, and carpal and tarsal bones; the third include the skull, sternum and ribs; and the fourth includes the bones of the vertebral column, which will be discussed in more detail in the next part of this chapter [5].

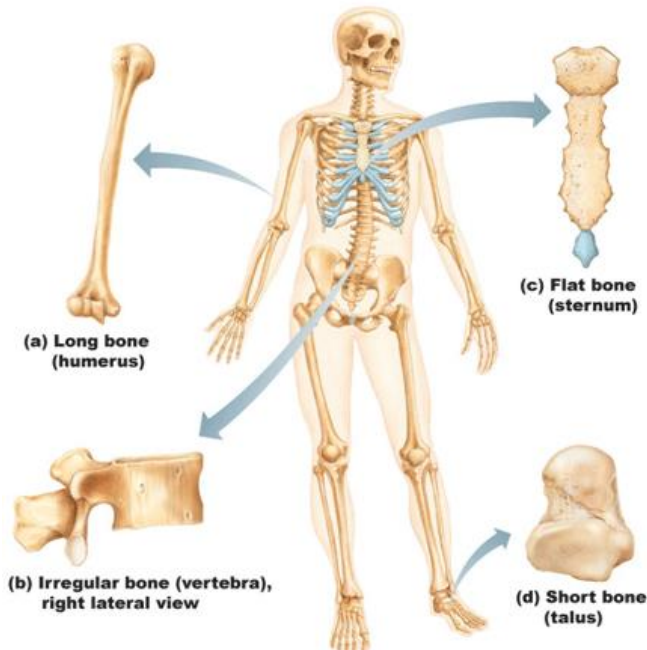


Figure 1. Human skeleton with examples of the four bone types [73]

2.2 Microstructural Anatomy

Long bones such as the tibia and femur are made up of two distinct regions named the diaphysis and metaphysis regions. The diaphysis is described as the hollow shaft, composed of mostly cortical bone, whereas the metaphysis bone is often cone shaped, and situated below the growth plates of the bones (Fig 2). Its makeup is of trabecular bone, surrounded by a thin covering of cortical bone (Fig 3). Different areas of the skeleton are made up of different ratios of cortical to trabecular bone. Although the human skeleton as a whole is made up of 80% cortical and 20% trabecular bone, the vertebra, for example, have a ratio of 25:75, whereas the femoral head is about 50:50 [5]. Such changes in ratios create uniqueness in the bone's properties and strength.

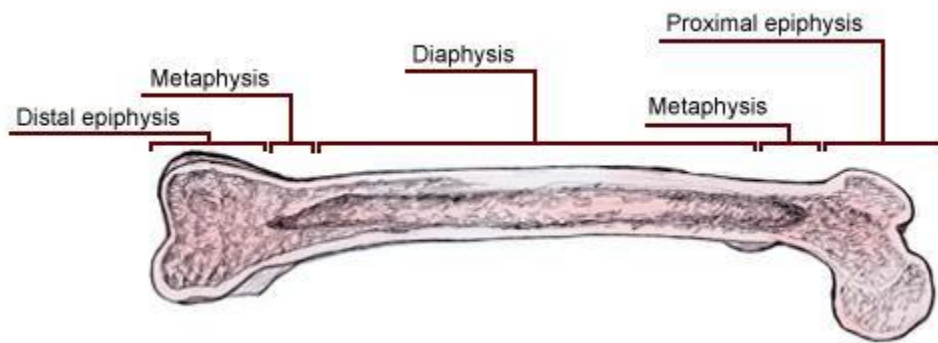


Figure 2. Diagram of a femur bone, with the diaphysis and metaphysis marked [6]

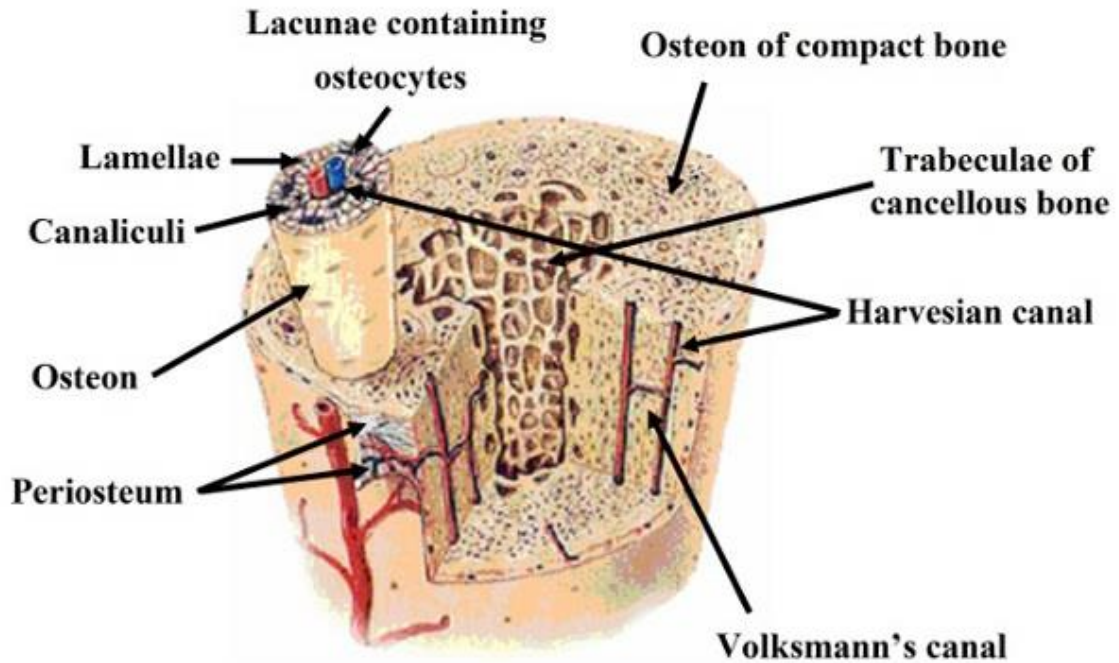


Figure 3. Diagram of metaphysis region with outer cortical and inner trabecular bone [7]

2.2.1 Cortical bone. Cortical bone is the denser of the two, providing protection for and encasing the inner bone marrow. Two surfaces, an outer periosteal and an inner endosteal, function to help remodel bone. The outer surface has higher rates of bone formation than resorption, leading to an overall increase in bone diameter as one ages. Increased formation allows the periosteal to provide better repairs during bone fracture. The osteons, or units, of cortical bones make up Haversian systems (Fig 2, above) [5]. Osteons surround a vessel which travels through the bone, known as the Haversian canal. Volkmann canals connect with the Haversian canals, allowing a more complex network for nerves to enter and blood to travel. These complete systems make long cylinders made up of concentric lamellae, and form networks within the cortical bone. The

lamellae represent the aged, absorbed osteons, and can act as a barrier to separate individual osteons units [5,6].

2.2.2 Trabecular bone. Trabecular bone, also known as cancellous bone, is much less dense. It is made up of a web or honey-comb like network of trabecular plates, broad and flat in shape, and rods, cylindrical in shape, where much of the bone marrow resides [6]. The osteons of trabecular bone are semi-lunar in shape and known as packets. The medullary cavity delivers much of the nutrients to trabecular bone, which is lamellar in nature. It's lamellar, or layered, structure allows for a glycoprotein layer to provide better adherence for osteoblasts during bone formation [5, 6].

2.2.3 Bone growth and resorption. Childhood and adolescence sees a major growth of bone, with both longitudinal and radial growth. While bone growth halts when one enters into adulthood, bone modeling and remodeling are constantly happening due to intrinsic and extrinsic variables. Bone modeling occurs as bones change their shape due to mechanical forces. Exercise and therapy types, as will be discussed in chapter 3, are ways to impart mechanical forces onto the bones, signaling for modeling to take place. This is commonly seen in long bones such as the femur and tibia, where such bones can change their overall shape in response to loads and forces. In standard bone modeling, bone formation and resorption should be near equal levels [5].

In conjunction with bone modeling, bone remodeling aids in the renewal of bone to maintain one's bone strength and density. Old bone is also resorbed during remodeling to prevent unnecessary bone accumulation. Figure 4 summarizes the four phases of bone remodeling, and will now be discussed in detail. Activation of osteoclasts begins the first

step in remodeling [5]. Osteoclasts originate from stem cells that undergo multiple mutational steps to form a multinucleated osteoclast. In charge of resorbing bone, upon activation it can move along bone surfaces via attachment proteins until it undergoes apoptosis, or cell death, about three weeks later [6]. Bone resorption is often characterized as the second step in remodeling.

The third step is known as the reversal stage, due to bone resorption giving way to bone formation. Cavities left in the bone from resorption contain preosteoblasts, along with monocytes and osteocytes. As osteoblasts are formed, reversal gives way to the fourth step of formation. Similar to osteoclasts, osteoblasts are also originated from stem cells. Through a series of reactions and steps, mesenchymal marrow stromal cells become osteoblasts. Osteoblasts can synthesize collagen fibers and proteins, enabling the formation of new osteoids or bone components [6]. The average span of formation via osteoblasts lasts about 100 days for each cell; following maturation of the cell, they become buried in the extracellular matrix of cortical bone and evolve into osteocytes. Osteocytes are the most common bone cells in the body, and can survive for decades forming networks. They keep their connection with each other and the bone surface through metabolic links of connexins. The cells also help transmit different mechanical stress signals [5]. The entire remodeling process can take up to 6 months to complete.

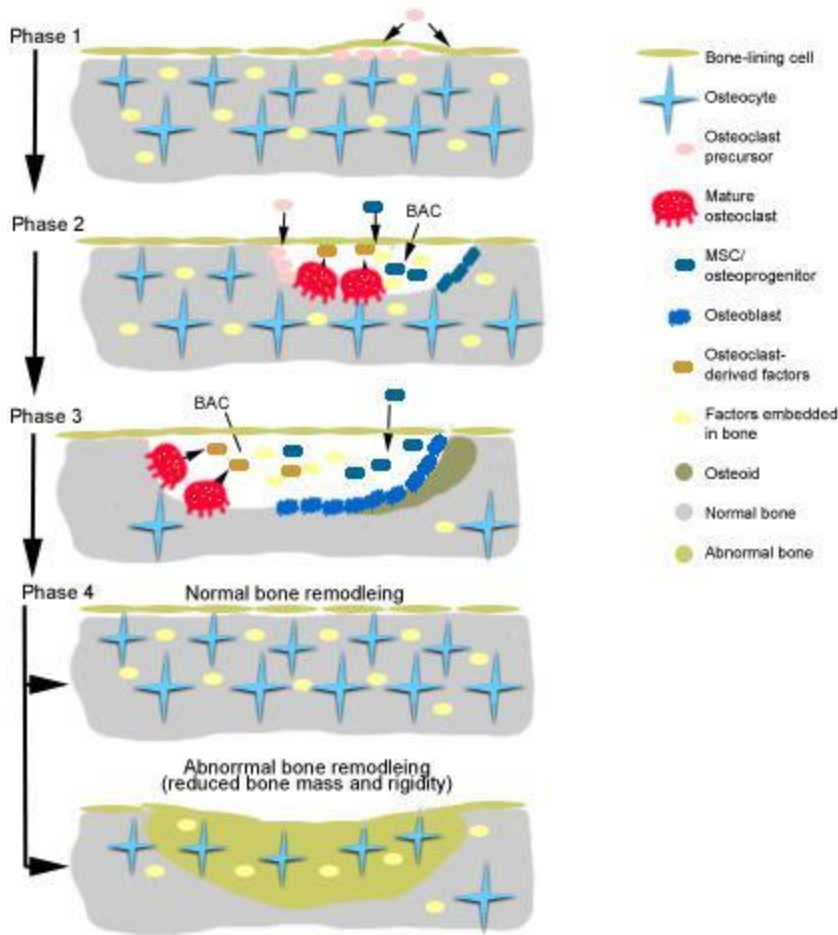


Figure 4. Diagram of four remodeling stages, with phase 1 activation, phase 2 resorption, phase 3 reversal and phase 4 formation [6]

Though it will be discussed in more detail in relation to SCI and rehabilitation in chapters 3 and 4, respectively, it is worth mentioning now the affects injury, and immobilization from it, along with exercise have on bone remodeling. In normal healthy adults, the absorption process and formation process of bone remodeling work at near equal levels to ensure that no bone degeneration is taking place, and that regular bone turnover is occurring. As mentioned, mechanical stresses subjected onto the bone, found in many active therapy and training techniques, help stimulate the process of bone

formation. However, following SCI in many individuals, they are not able to move their limbs to stimulate any force or stress upon the bone. Especially seen in the long bones of the hind limbs, the femur and tibia loses much of its density as resorption begins to take over any new bone formation. Trabecular bone is especially susceptible to bone degradation, as the denser cortical bone tends not to lose as much density over time [8]. Because bone loss leads to easier fracture and injury, therapeutic and rehabilitation techniques are important to those following SCI to help them activate the mechanical stress signals in the bone when the individual cannot do so themselves. As we will see in Chapter 4, both passive and active training methods are currently being utilized to help stimulate bone formation and reduce regeneration that takes place following injury [33,52,54].

2.2.4 Tibia anatomy. Following the femur, the tibia is the second largest bone in the body (Fig. 5). The proximal, or femur end of the tibia has a medial and lateral condyl that articulates with the femur to form a part of the knee joint. The body of the tibia is triangular in cross section, with a medial, lateral, and posterior border. The lower end of the tibia has a process that juts out known as the medial malleolus, and along with the fibula and group of talus bones, form the ankle joint. The shaft or body of the tibia is mainly comprised of cortical bone, but the amount of trabecular bone increases towards the medial compartment of the proximal tibia. Here, trabecular bone can be seen to decrease depending on bone disease, age, or inactivity [10]. Such diseases as osteoporosis, that degenerates bone can cause trabecular pattern loss, decreasing the bone density [9].

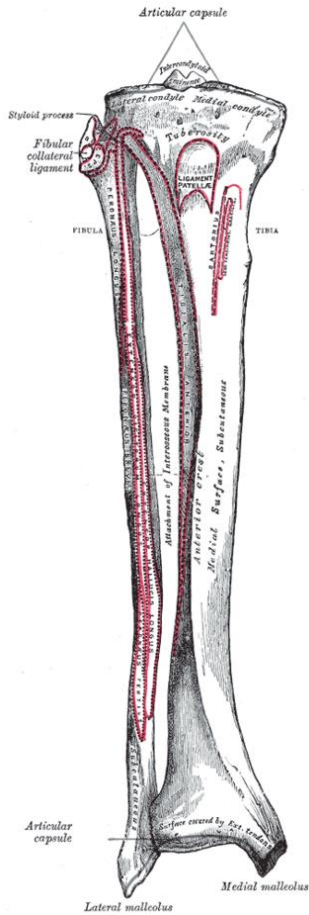


Figure 5. Anatomy of the tibia [11]

2.3 The Spine

2.3.1 The vertebral column. The vertebral column, or more commonly known as the backbone, is comprised of 33 vertebrae making up four regions of the spinal column. Starting from the top of the spinal cord, the first region is known as the cervical spine, followed by the thoracic spine, lumbar spine, the sacrum, and the coccyx (Fig. 6). The vertebral body and vertebral arch are the two main components of the spine. The vertebral body is made up of the centrum, situated anterior to the body and comprised of

trabecular bone with a thin cortical outer layer, while the vertebral arch is posterior to the body and has a thicker cortical covering (Fig. 7).

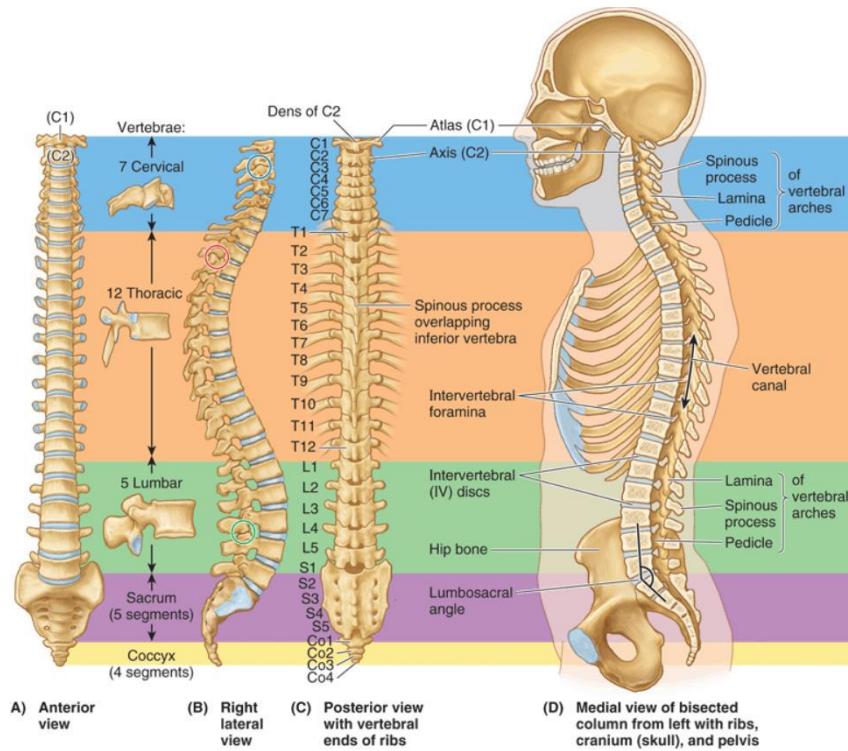


Figure 6. The five regions of the vertebral column [14]

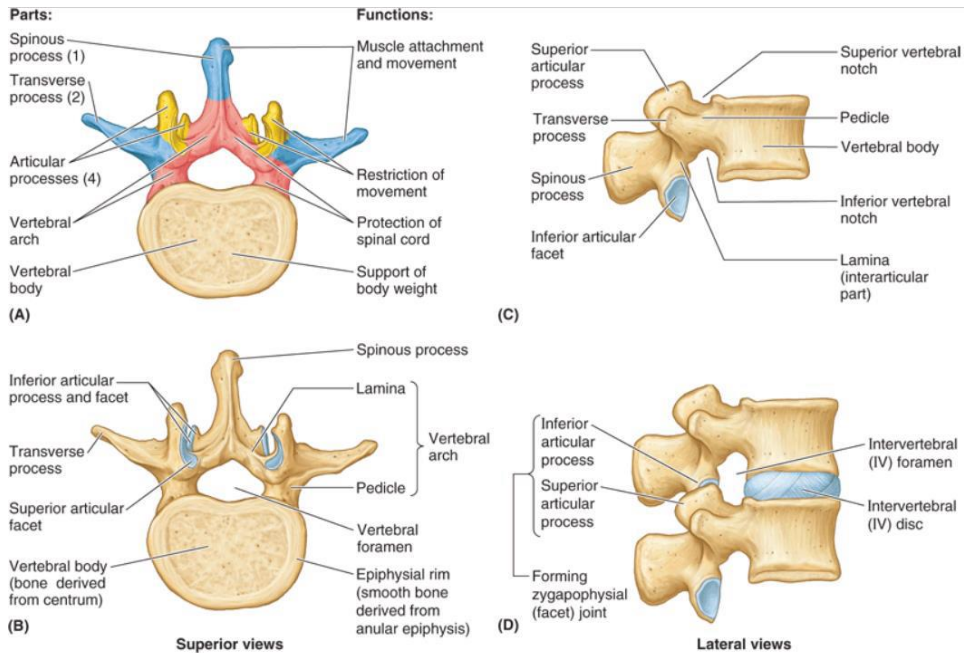


Figure 7. Superior and Lateral views of the lumbar vertebra, made up of the vertebral body and arch [14]

The top and bottoms of each vertebra body are fairly flat and rough in texture, known as the endplates, helping for the adhesion of the intervertebral discs in between each bony vertebra (Fig. 7, above). The endplates, besides adhesion, also help to distribute loads evenly, and can even act as a water and solute exchange interface. The vertebral arch is formed by two pedicles, short bony processes, which extend posterior from the bone. Along each pedicle, a lamina acts to join the vertebral arch and from a posterior border, as seen in (b) of Fig. 7, above.

The intervertebral discs are made of an outer ring, known as the annulus fibrosus disci intervertebralis, and a center, known as the nucleus pulposus (Fig. 8). The outer annulus has several fibrous layers of both type I and type II collagen, enabling it to withstand greater compressive forces. The inner nucleus, on the other hand, is made up of

looser fibers and helps distribute such forces evenly across the disc. If pressure were not to be distributed and focused in the load area, this could cause damage to the underlying endplate of the vertebra [14]. Common intervertebral disc problems are hernias, degeneration, and scoliosis.

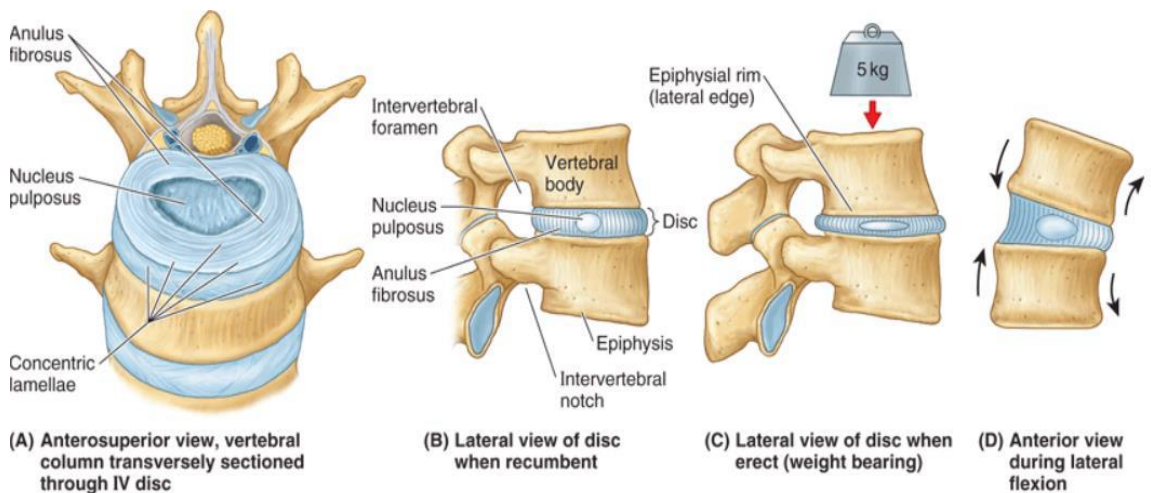


Figure 8. Different views of the vertebral discs and their anatomical components and functions to load [14]

The cervical vertebrae is made up of seven bones (C1—7), making up the neck of humans. Their bodies are small, with narrow laminae and short spinous processes; the first vertebrae, C1, also known as the atlas, form the piece connecting the skull and the spine. Unlike all other vertebrae, the atlas has no vertebral body, being fused directly to the C2, or axis vertebra. The axis forms a pivot that allows the atlas to rotate and give a great range of motion to support and move the skull. The last cervical vertebra, C7, also known

as the vertebra prominens, has a long spinous process, which can usually be seen and felt at the base of the neck [14].

The thoracic vertebrae makes up a large center portion of the column of 12 total vertebrae (T1—12), with the first connecting to the final cervical (C7) vertebrae and the twelfth connecting to the first lumbar (L1). The thoracic vertebrae have broad bodies with the pedicles directed backwards and slightly upwards. Laminae are also broad, and the spinous processes long, stemming from the lamina and sprouting downwards. The first vertebra, T1, has a specific and unique facet and portion of a second facet where the first and second ribs are connected. Its spinous process sticks out more horizontally than the others. As one moves down the thoracic spine, the vertebrae bodies can be seen to get slightly larger. The T11 vertebra has a short and almost horizontal spinous process, and is close in size to the lumbar vertebrae. The final T12 vertebra closely resembles those of the lumbar spine, with its spinous process, body, and laminae closer than those of its fellow thoracic vertebrae [14].

The lumbar vertebrae connect the thoracic spine to the Sacrum, and is made up of five (L1—5) vertebrae. Being the largest of the vertebrae, the lumbar spine helps support the weight of the body and movement of the core. The lumbar body is large and wide, with thick pedicles that eject backwards that increase in angulation as one moves down the spine. The laminae are shorter but broad, and jut out from the posterior of the vertebral arch. The spinous process is also broad and projects backwards, with a rough notch at its end. While the majority of individuals have five lumbar vertebrae, there are some that have four or six [14].

Beginning with the sacrum, the bones are fused with no intervertebral discs in between. The sacrum is a large bone made up of five attached segments (S1—5). The base of the sacrum is directed up and forward, with one large projection on each side known as the ala of sacrum. The middle of the base is an oval shaped surface, with the sacral canal situated behind it along with its lamina and spinous processes of the first sacral vertebra. The pelvis side is concave in shape and broad; four horizontal ridges, representing what was once the five separated vertebrae, run transverse along the surface. The dorsal surface is convex and narrower, with a median sacral crest running down its middle. Rudimentary spinous processes jut out from the S3 and S4 vertebrae. As with the lumbar spine, some individuals have four or six sacrum vertebrae instead of the more commonly seen five [14].

The coccyx, also referred to as the tailbone, represents the last vertebral column in humans, made up of five fused vertebrae (Co1—5). The first three segments follow the shape of a rudimentary vertebra body, with the final vertebra a bone nodule. None of the coccyx vertebrae have pedicles, laminae, or spinous processes, with their size diminishing as one moves towards the end. In human adults, it is possible that not all of the coccyx is fused, with two or three separate segments being possible. While a remnant of a vestigial tail, it is still important for the attachment of muscles, ligaments and tendons, along with offering support in both standing and sitting positions [14].

The shape of the spinal column is unique depending on the region. The first cervical curve, a slight convex projection forward, begins at the axis (C2) and ends at the T2 vertebra. The thoracic curve then begins concave forward, beginning where the cervical curve ends and extending to the T12 vertebra. The lumbar curve follows, starting

at the T12 and is convex in curvature, ending at the final sacral curve. The sacral curve is concave, and ends at the beginning of the coccyx. The cervical and lumbar curves become more prominent as one matures, and are denoted as ‘secondary’ curves, compared to the ‘primary’ lumbar and sacral curves which are present in-utero.

The rat spinal column is quite similar to that of humans, with the dimensions of the cervical and lumbar spine being exceptionally close in anatomical ratios (Fig. 9). The spinal canal width to depth ratio is similar at all levels between species. More flexibility is seen with rat spines, with lumbar differences more apparent from being a quadruped versus biped [15].

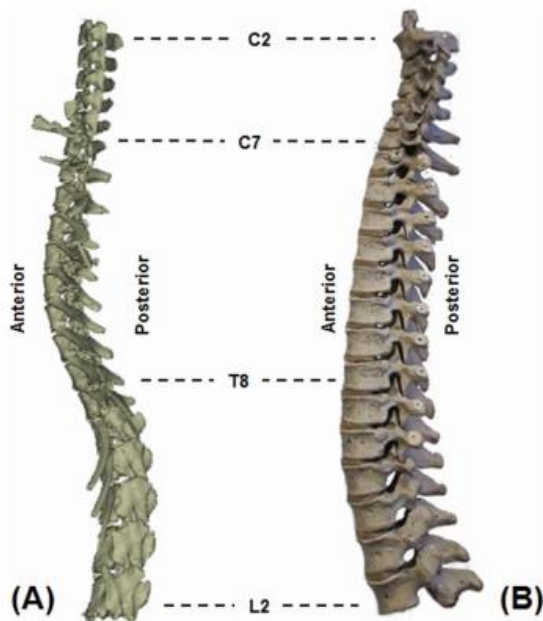


Figure 9. Lateral view comparison of (A) rat and (B) human spinal column from the C2—L2 levels [15]

2.3.2 The spinal cord. The spinal cord is the bundle of nerves that runs from the medulla oblongata, or the hindbrain that controls all autonomic functions, to the lumbar spine. It is protected by the spinal (vertebral) column, and functions to transmit neural signals and firing from the brain to the body and back, as well as having its own unique neural reflexes. Specifically, the spinal cord begins at the opening in the occipital bone at the base of the skull known as the foramen magnum; numerous arteries also pass through this opening. For most humans, the spinal cord ends at the L2 vertebra in a fibrous bundle known as the filum terminale. Underneath the spinal column is the dura mater layer, underlying a small void known as the epidural space that is filled with adipose tissue (Fig. 10). The next layer is the arachnoid mater, with a subarachnoid space, and finally the pia mater that is directly encasing the spinal cord. Along with the brain, the spinal cord is a part of the central nervous system (CNS) [14].

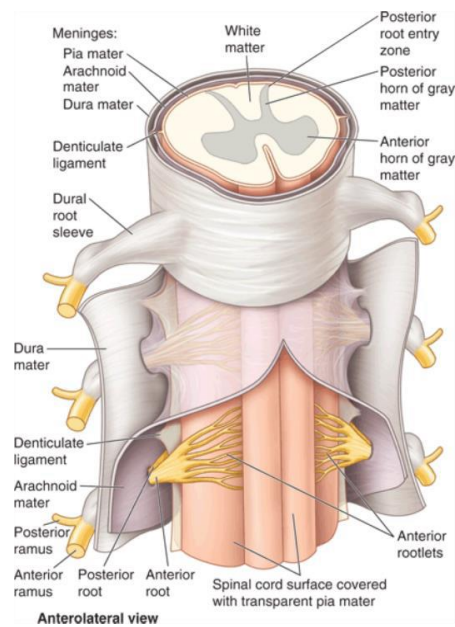


Figure 10. Diagram of cross section of the spinal cord and its protective layers [14]

Thirty-one segments construct the spinal cord, each containing a sensory nerve and motor nerve root. Nerve roots come together to form 31 pairs of nerves, which begins the peripheral nervous system (PNS). Axons of the spinal cord are able to receive sensory information from all parts of the body. When bundles of axons, or fascicles, are formed, they are called dorsal roots. Ventral roots are also a part of the spinal cord, known as efferent fibers that only project signals away from the spinal cord. All the pairs formed by these unique roots branch off at the segments in an orderly pattern—for example, the ventral and dorsal roots from the spinal nerves. At the center of the cord sits the grey column, comprised of motor neurons, interneurons, and unmyelinated (uninsulated) axons. On the exterior of the grey column is the white matter, made up of myelinated, or insulated, axons (Fig. 10, above).

In the cervical vertebrae region, there are eight pairs of cervical nerves. An enlarged segment, from about the C4—T1 region of the spinal column, is known as the brachial plexus and connects afferent nerves, which bring signals back to the CNS, and efferent nerves to much of the upper body. Twelve thoracic segments follow, forming pairs of thoracic nerves. The lumbar contains five segments and pairs of lumbar nerves, where another enlargement is located known as the lumbo-sacral enlargement. The bundle of nerves, or lumbosacral plexus, innervates much of the lower limbs and runs from the T9—T12 vertebrae, corresponding to the L2—S3 spinal cord segments. After the lumbar segments are five sacral segments and pairs of sacral nerves, and lastly 1 coccygeal segment. Figure 11 diagrams all the separate 31 segments of the spinal cord [14].

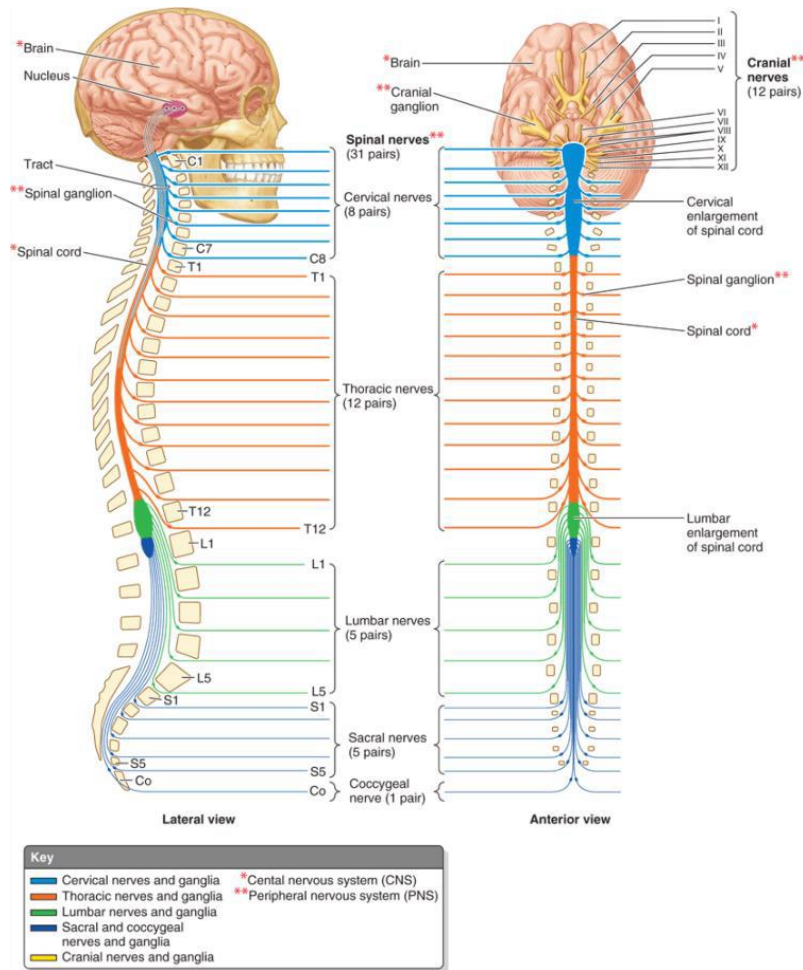


Figure 11. Diagram of the 31 segments of the spinal cord [14]

2.3.3 Spinal cord injury. Due to the complexity of the spine, and the important role it plays in transmitting and receiving messages to and from the rest of the body, injury to it can lead to a wide array of outcomes, some more traumatic than others. Worst case, severe injury to the spinal cord can lead to death. While the most common cause of SCI is from mechanical or physical trauma, including car accidents, falls, or sports related injuries, other causations include spinal cord diseases and tumors which can lead to severe injury and degeneration of the spine [1]. Once the injury has occurred, primary

damage begins taking effect on the body. Blood vessel damage, contusions, and cell and axon death directly from the accident are immediate. Unfortunately, since the primary damage takes place so quickly, very little preventative measures can be undertaken to minimize damage. Secondary damage, indirectly caused from the injury, can be better minimized. Keeping an adequate blood supply to the area, along with medications and physical therapies at a later time point can reduce secondary damage. Secondary damage includes ischemia from lack of blood flow, hypoxia from lack of oxygen, increase of pressure to the injury, and infections [16].

The two most basic descriptions of SCI are diagnosing them as ‘incomplete’ or ‘complete’. Complete SCI are classified when the individual has no voluntary motor function below that of the injury site. However, there is some ambiguity over what is truly classified as complete injury or not. For example, some injured individuals may have minimal function in areas below that of the injury site, but just not any sensory function; or, they may have minimal function on one side of the injury but not the other. The American Spinal Injury Association (ASIA) adopted a classification system in grading the impairment of patients with SCI [17]. Graded from A to E, it is a measure of neurological loss seen in the anatomy below the sacral region. The sacral region was selected, or specifically, the S4—5 vertebra, to be the new level threshold when defining complete vs. incomplete SCI. This is because very few patients with injury to the sacral site experienced any partial sided function or recovery as those with injuries higher up. So, when looking for completeness, only function from the S4—5 and down is measured. This was followed in the ASIA impairment scale. The highest level, A, is the only complete injury on the scale, with levels B through D ranging from severe to mild

incomplete injury. E is categorized as normal motor and sensory function [17]. ASIA also has a scale in grading the functionality of muscles after SCI, ranging from 0—5*. All grading scales can be seen in detail in Figure 12.

Muscle Function Grading

- 0 = total paralysis
- 1 = palpable or visible contraction
- 2 = active movement, full range of motion (ROM) with gravity eliminated
- 3 = active movement, full ROM against gravity
- 4 = active movement, full ROM against gravity and moderate resistance in a muscle specific position
- 5 = (normal) active movement, full ROM against gravity and full resistance in a functional muscle position expected from an otherwise unimpaired person
- 5* = (normal) active movement, full ROM against gravity and sufficient resistance to be considered normal if identified inhibiting factors (i.e. pain, disuse) were not present
- NT = not testable (i.e. due to immobilization, severe pain such that the patient cannot be graded, amputation of limb, or contracture of > 50% of the normal ROM)

Sensory Grading

- 0 = Absent
- 1 = Altered, either decreased/impaired sensation or hypersensitivity
- 2 = Normal
- NT = Not testable

When to Test Non-Key Muscles:

In a patient with an apparent AIS B classification, non-key muscle functions more than 3 levels below the motor level on each side should be tested to most accurately classify the injury (differentiate between AIS B and C).

Movement	Root level
Shoulder: Flexion, extension, abduction, adduction, internal and external rotation	C5
Elbow: Supination	
Elbow: Pronation	C6
Wrist: Flexion	
Finger: Flexion at proximal joint, extension	C7
Thumb: Flexion, extension and abduction in plane of thumb	
Finger: Flexion at MCP joint	C8
Thumb: Opposition, adduction and abduction perpendicular to palm	
Finger: Abduction of the index finger	T1
Hip: Adduction	L2
Hip: External rotation	L3
Hip: Extension, abduction, internal rotation	L4
Knee: Flexion	
Ankle: Inversion and eversion	
Toe: MP and IP extension	
Hallux and Toe: DIP and PP flexion and abduction	L5
Hallux: Adduction	S1

ASIA Impairment Scale (AIS)

A = Complete. No sensory or motor function is preserved in the sacral segments S4-5.

B = Sensory Incomplete. Sensory but not motor function is preserved below the neurological level and includes the sacral segments S4-5 (light touch or pin prick at S4-5 or deep anal pressure) AND no motor function is preserved more than three levels below the motor level on either side of the body.

C = Motor Incomplete. Motor function is preserved at the most caudal sacral segments for voluntary anal contraction (VAC) OR the patient meets the criteria for sensory incomplete status (sensory function preserved at the most caudal sacral segments (S4-S5) by LT, PP or DAP), and has some sparing of motor function more than three levels below the ipsilateral motor level on either side of the body. (This includes key or non-key muscle functions to determine motor incomplete status.) For AIS C – less than half of key muscle functions below the single NLI have a muscle grade \geq 3.

D = Motor Incomplete. Motor incomplete status as defined above, with at least half (half or more) of key muscle functions below the single NLI having a muscle grade \geq 3.

E = Normal. If sensation and motor function as tested with the ISNCSCI are graded as normal in all segments, and the patient had prior deficits, then the AIS grade is E. Someone without an initial SCI does not receive an AIS grade.

Using ND: To document the sensory, motor and NLI levels, the ASIA Impairment Scale grade, and/or the zone of partial preservation (ZPP) when they are unable to be determined based on the examination results.



Steps in Classification

The following order is recommended for determining the classification of individuals with SCI.

1. Determine sensory levels for right and left sides.

The sensory level is the most caudal, intact dermatome for both pin prick and light touch sensation.

2. Determine motor levels for right and left sides.

Defined by the lowest key muscle function that has a grade of at least 3 (on supine testing), providing the key muscle functions represented by segments above that level are judged to be intact (graded as a 5).

Note: in regions where there is no myotome to test, the motor level is presumed to be the same as the sensory level, if testable motor function above that level is also normal.

3. Determine the neurological level of injury (NLI)

This refers to the most caudal segment of the cord with intact sensation and antigravity (3 or more) muscle function strength, provided that there is normal (intact) sensory and motor function rostrally respectively.

The NLI is the most cephalad of the sensory and motor levels determined in steps 1 and 2.

4. Determine whether the injury is Complete or Incomplete.

(i.e. absence or presence of sacral sparing)
If voluntary anal contraction = No AND all S4-5 sensory scores = 0 AND deep anal pressure = No, then injury is Complete.
Otherwise, injury is Incomplete.

5. Determine ASIA Impairment Scale (AIS) Grade:

Is injury Complete? If YES, AIS=A and can record ZPP (lowest dermatome or myotome on each side with some preservation)

NO ↓

Is injury Motor Complete? If YES, AIS=B

NO ↓

(No=voluntary anal contraction OR motor function more than three levels below the motor level on a given side, if the patient has sensory incomplete classification)

Are at least half (half or more) of the key muscles below the neurological level of injury graded 3 or better?

NO ↓

AIS=C

YES ↓

AIS=D

If sensation and motor function is normal in all segments, AIS=E

Note: AIS E is used in follow-up testing when an individual with a documented SCI has recovered normal function. If at initial testing no deficits are found, the individual is neurologically intact; the ASIA Impairment Scale does not apply.

Figure 12. ASIA grading scales for neurological impairment (boxed, center) and muscle function (top left) along with incomplete vs. complete classification (right) [18]

Depending on where the injury occurs in the spinal cord, different impairments can be seen. Generally, the higher the injury is in the spine, the more areas are affected in the body. Beginning with the lower parts of the spine, lumbosacral injuries result in the

least impact on immobility or paralysis in the body. Lack or loss of control in the legs and hips may be present including the inability to flex the thigh or extend the leg. L4—5 injuries may have knee and foot flexion loss, and S1—2 injuries may cause loss of plantar foot and toe flexion, along with hip extension. Since much of the functions of the bowels and lower regions are innervated in the sacral spine, bladder dysfunction is common [19].

Injuries at the thoracic levels may see paraplegia, or paralysis in the legs and lower limbs if complete, including all lumbosacral injury effects. Injuries occurring at the T1—8 levels result in immobility of the abdominal and chest muscles. Injuries at T9—12 levels may see varying degrees of abdominal muscle control. The higher the thoracic injury is, the greater chance of the individual having thermoregulation and high blood pressure problems [20]. Especially prominent in injury above the T6 level is autonomic dysreflexia and neurogenic shock. Dysreflexia is a result in the overstimulation caused by sudden high blood pressure to the nervous system, while neurogenic shock results from sudden low pressure. Both can lead to death if not treated [21, 22].

Injuries to the cervical spine, around neck level, may result in degrees of tetraplegia, in which at least the arms and legs lose sensation and have little to no controlled movement, if not complete paralysis. All symptoms from injuries of the thoracic and lumbosacral regions are present. Thermoregulation may be an issue, along with maintaining normal blood pressure and heart rate. Beginning with the C1—4 region, if one were to suffer complete SCI, it becomes impossible to breathe without some ventilation system. The C5—6 region sees the paralysis of the wrists, triceps, and hands, along with much difficulty breathing. Some patients with injuries in the lower C7—8

region may be able to move their hands, but grasping and controlled movement is difficult [23].

2.3.3.1 Spinal cord injury in animal models. In rat SCI models, different surgical techniques can be implemented to induce injury. Table 1.1 below summarizes the four main types of injury models utilized. Hemi-sections, compression, and contusion types are used to simulate incomplete SCI, while transections are commonly used to model complete SCI. For our current study, a moderate contusion at the T9—10 site in rats was given via a weight drop system, as described in Chapter 4. The weight drop system can be adjusted to induce a mild to severe injury by changing the weight itself, or the height from which it is dropped.

Table 1

Description of the numerous SCI animal models used in spinal research to simulate human SCI [24]

Model	Description	Advantages/Disadvantages
Contusion	Induced with an impactor i.e. weight-drop from a Specified height (Allen, 1911), thoracic contusion is most commonly used (Behrmann <i>et al.</i> , 1993; Jakeman <i>et al.</i> , 2000) Clip Induced with clips calibrated to exert a force of 50/35g-	Impact from contusion can be difficult to assess pain behaviour due to variation of distance
Clip compression	Induced with clips calibrated to exert a force of 50/35g -50g = severe response and 35g = moderate response The clip is closed over the entire cord for 1 minute (Bruce <i>et al.</i> , 2002)	Allows for precise control of injury Does not resemble injury seen in humans
Balloon compression	Uses different volumes of balloon inflation and different compression durations of expression to create contusion (Lim <i>et al.</i> , 2007)	Controlled environment Non-invasive method of creating SCI
Computer controlled contusion	Uses an animal trap that delivers a set weight to the exposed spinal cord; the computer monitors the (Stokes and Jakeman, 2002)	Reproducible, controlled environment But equipment is expensive
Spinal cord displacement	impact attempts to regulate trauma impact by Controlling displacement length of the spinal cord (Nakae <i>et al.</i> , 2011)	Controlled displacement and monitoring of biochemical parameters at the time of impact helps reduce outcome variability-controlled environment
Transection	Complete spinal transection, performed using spring scissors (Kang <i>et al.</i> , 2011; Nakae <i>et al.</i> , 2011)	Widely used to assess regeneration (Talac <i>et al.</i> , 2004) but it is clinically irrelevant (Poon <i>et al.</i> , 2007)
Photochemical	The use of a dye induces the photochemical reaction by activating an argon laser to produce single oxygen molecules on the endothelial surface of spinal cord vessels (Watson <i>et al.</i> , 1986)	Reliable and reproducible Does not induce mechanical trauma to the cord Extent of injury is difficult to control
Excitotoxic	Intraspinal/intrathecal injection of excitotoxins e.g., quiscolic acid (Bhatoo, 2009)	Long-lasting spontaneous pain, thermal hyperalgesia and mechanical allodynia (Fairbanks <i>et al.</i> , 2000; Yezierski <i>et al.</i> , 1998) Has ability to correlate specific areas of tissue damage
Spinothalamic tract lesions	Lesions core pain pathway; spinothalamic tract area using tungsten microelectrode (Nakae <i>et al.</i> , 2011; Zeilig <i>et al.</i> , 2011)	Resembles allodynia and hyperalgesia Provides useful and novel insights into the underlying biological mechanisms of SCI
Canal stenosis	Is entrapment of the cauda equine and/or lumbar Nerve roots by hypertrophy of osseous and soft tissue structures surrounding the lumbar spinal cord that reduces blood flow (Sekido <i>et al.</i> , 2012)	This model helps clarify pathophysiology of chronic, light pressure to the spinal cord (Sekiguchi <i>et al.</i> , 2004)

Chapter 3

Bone and Muscle Changes Following Spinal Cord Injury (SCI)

3.1 Introduction

SCI individuals commonly experience muscle atrophy and bone loss. Due to such degradation, further injury to the legs such as fractures can be frequently seen in these individuals. The amount of muscle atrophy and bone loss is dependent upon numerous variables, including the severity of the SCI, as well with the amount of time one goes without any rehabilitation and therapeutic procedures [2]. From the reduction in mechanical loading placed upon the limbs and muscles after injury, atrophy and osteoporosis can be seen. Certain measurements, including the mass of the muscle and the bone microstructure properties of both cortical and trabecular bone, along with others, are commonly studied in SCI individuals to compare with those of uninjured and get a better understanding of the changes that occur after injury to the limbs. Biomechanical tests, like three-point bending on bones of that below the injury site can also generate results which are normally studied in animal models of SCI. While passive and active training, as will be further discussed in later chapters, can help minimize, if not reverse, such bone and muscle damage or atrophy, it is pertinent to understand the changes that occur in the bones and muscles that take place following SCI.

3.2 Muscle Atrophy Morphology

Muscle atrophy can be simply characterized as a decrease in mass of a muscle (Fig 13). Any prolonged period of inactivity can lead to a loss of muscle mass, since no force is exerted on it. At any given moment, there is a checks-and-balances system in

place between the regulation of protein synthesis and protein degradation. In a normal individual with no need for inactivity, this system is working properly such that one does not overtake the other. In individuals who exercise frequently, protein synthesis can overtake degradation, leading to an increase in muscle mass and growth. Contrarily, individuals with loss of movement and no ability of mechanical movement, such as those with SCI, have their protein degradation pathways drastically overtaking any protein synthesis. The protein degradation pathway has been seen to be ATP-dependent, relying on four copies of ubiquitin, a regulatory protein, to ligate onto a substrate protein. Once this has occurred, a proteasome is able to recognize its need for the substrate protein to be degraded [25].

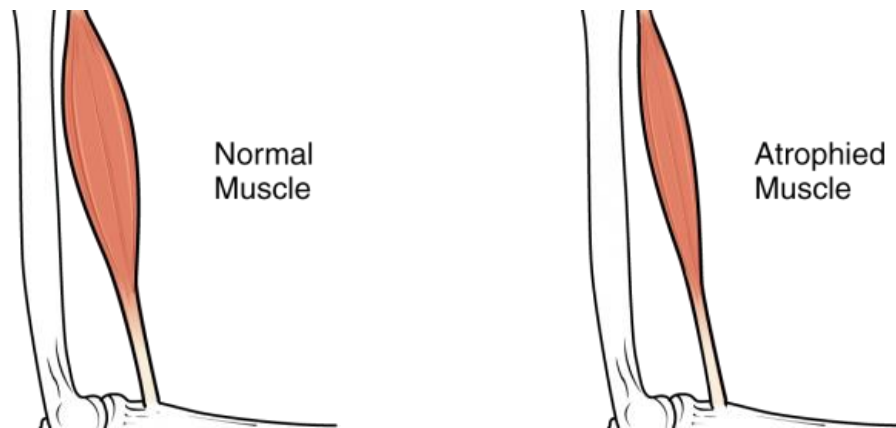


Figure 13. Drawing of a healthy, normal muscle (left) and a muscle undergoing atrophy (right) [71]

Muscle loss may lead to a decrease in metabolic rate due to changes in body composition. Glucose intolerance, insulin resistance, hyperlipidemia, and numerous other cardiovascular diseases may result from reduced metabolic functions, and the weight gain

often associated with it [26]. Serving as the mechanical stimulus for bone loading and movement, muscle atrophy is an important factor in maintaining bone density as well. Rehabilitation and training are vital in persons to preserve muscle mass.

3.3 Bone Loss Morphology

Bone loss is seen in the loss of bone density, or bone mineral density (Fig 14). In a healthy individual, calcium and phosphate, along with other minerals we absorb from foods or supplements, are utilized to help build new bone. As we begin to age, it is natural for the body to reabsorb bone faster than it is replenished. However, in individuals that are unable to use their limbs, regardless of age, bone loss is seen from the lack of mechanical loading placed upon the limbs.

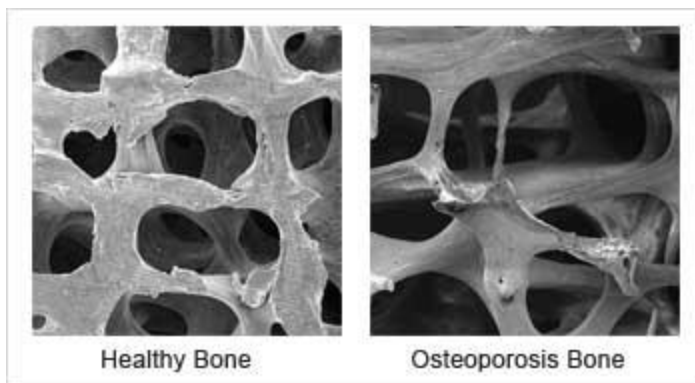


Figure 14. Bone density scan of a normal bone (right), and one that is osteoporotic and incurred bone loss (left). [42]

Fractures, and the complications stemming from such fractures, are more commonly seen in SCI patients with bone loss, having about a doubled increased risk

than non-SCI individuals [27]. Osteoporosis sets in at far greater levels at bone sites below that of the injury compared to being caused by more standard factors such as aging, hormonal changes, or bed rest [28]. Infections, skin sores, and misaligned healing can be seen as additional problems that can be caused by bone loss. Specifically, bone loss can also lead to such problems as osteoporosis, hypercalciuria, renal uretolithiasis, and bladder stones [29]. This is related to the extra exertion put onto the kidneys, attempting to filter excess degraded bio products of the bones and muscle. This bone resorption by the body is a contributor in the rapid bone loss shortly following SCI. Much like complications arising from muscle atrophy, this can be better prevented through rehabilitation training techniques.

3.4 Human Studies

3.4.1 Muscle changes. The magnitude of muscle atrophy can be seen in the muscle mass lost below that of the spinal injury site. All areas below this level are most affected, with reduced, if any, real ability to move in the injured individual. A study that followed fourteen patients with thoracic level injury from 6 to 24 weeks post SCI has shown that lower limb atrophy can be seen. At the initial six week mark, cross sectional areas of muscle below that of the injury site had displayed a reduction in mass between 18—46%, with additional declines in tissue differing depending on the muscle analyzed. By the 24th week, the gastrocnemius muscle saw a reduction of 24%, the soleus 12%, the quadriceps 16%, and the hamstrings 14% [30]. Incomplete SCI studies have shown results of a 30% reduction in cross sectional areas six weeks following injury, as well as a total of 43% in atrophy 4 to 5 months post SCI [31]. Comparing cross sectional areas between incomplete and complete thoracic SCI individuals to normal populations have

shown 23% and 28% reduction in calf muscle areas [32]. Overall muscle area can decrease by 34—39% in thoracic SCI patients [33].

Measurement of muscle mass can also showcase the atrophic changes occurring. One such study found a total hind limb muscle mass reduction of 15% one year following SCI [34]. Changes in muscle density have also been seen with both incomplete and complete thoracic SCI. Incomplete SCI patients saw a 13.2% lower calf muscle density, and complete SCI patients a 19.4% lower calf muscle density [32].

3.4.2 Bone changes. Bone loss differs depending on the type of bone tissue in question, though the majority of bone loss can be seen in the trabecular bone of the femur and tibia [8]. Cortical bone loss is reported, however, with overall area reductions about 25% lower than those of the normal, uninjured population [33]. Other variables measured, seen in cross sectional studies, have shown tibial trabecular, or cancellous, bone losses within the first two years following SCI to range anywhere from 0.4—80%, with tibial cortical bone losses only reaching a maximum on average of 32.7% in cross sectional area [35]. When measured monthly, cancellous bone experienced losses of 1—4% a month up to the first year. In another study looking at tibial bone loss, following six months after SCI, trabecular bone loss was calculated at 5%, and 15% one year post-SCI for paraplegics. The same study also calculated cortical bone loss to be 2% and 7% at six and 12 months, respectively. No significant differences were seen in subjects with tetraplegia [28]. Eventually, it has been studied that bone loss reaches a plateau at around 50—60% decline in bone mineral density [29].

In addition to overall bone cross sectional area, specific measured variables can be further investigated to provide a better understanding of bone loss. Bone volume over total volume, trabecular number, trabecular separation and cortical thickness are commonly recorded, with numerous studies showing that reduced bone volume, trabecular number and cortical thickness, and increased trabecular separation are seen in persons with SCI [2,74,75]. Trabecular bone properties in tibia of complete SCI patients had a 20% reduction in bone volume, 20% reduction in trabecular number, and 33% higher trabecular separation; femur properties were recorded with a 27% lower bone volume, 21% lower trabecular number, 44% higher trabecular separation, along with a 8% reduction in trabecular thickness [36].

The aforementioned variables are all important measurements of bone microstructure properties that provide useful comparisons when looking at SCI vs. non-SCI persons, and can be found through micro-computed tomography (micro-CT) and computed tomography analysis (CTAN) scanning and image reconstruction. Bone volume over tissue volume, also known as bone volume density, is a percentage measurement of the bone volume over the total volume (BV/TV%), indicating the fraction of bone in a particular volume of interest (VOI) being analyzed. It can be used to evaluate the changes that took place in the bone's volume density following a treatment, such as drug effects or implantations, or, in this case, an injury. Trabecular thickness (Tb.Th), trabecular separation (Tb.Sp), and trabecular number (Tb.N), are important measurements that can be used to study bone strength, and how such strength is altered via treatment or injury in trabecular bone. The trabecular thickness can be seen to measure how thick the trabecular structures are comprising the bone, with the trabecular

spacing, in turn, being the open areas comprised of no bone material (see Fig 15) [37]. As can be expected, bone undergoing loss from inactivity, from injury or otherwise, will lose some of its trabecular structure, creating more open gaps in the bone when scanned.

Trabecular number is often taken as the inverse of the mean distance between the central axis of the bone, measuring the average number of trabeculae found per unit of length (Fig 16). Standard unit of measurements for each variable is mm or μm for both Tb.Th and Tb.Sp, and $1/\text{mm}$ or $1/\mu\text{m}$ for Tb.N. Quite similar in definition to Tb.Th, cortical thickness (Ct.Th) is the average cortical thickness making up the cortical bone, also measured in mm or μm [38].

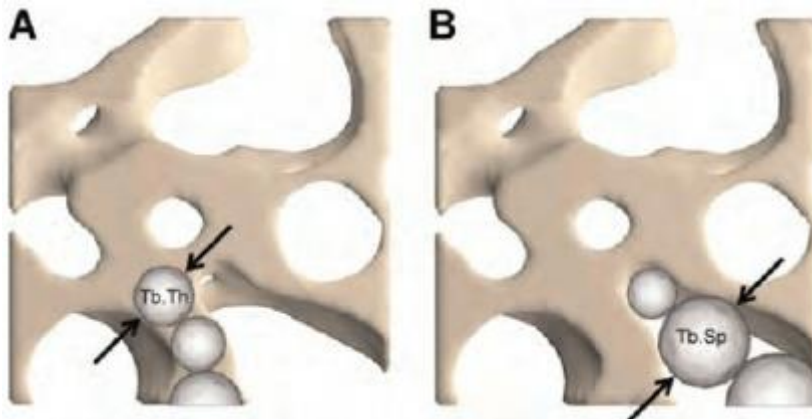


Figure 15. MicroCT image for calculating trabecular thickness (A) and separation (B). 3D distances computed by fitting spheres inside the background. The average diameter of the spheres represents the object thickness, and the standard deviation of the diameter represents the variability in the object thickness [39]

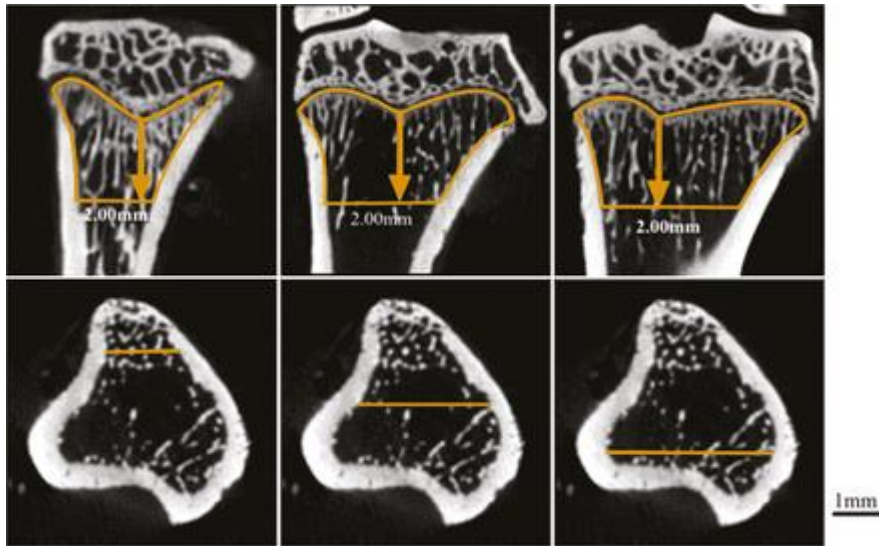


Figure 16. Comparison of axis for different planes (coronal, top and transverse, bottom) in calculating the number of trabecula in tibia bone [40]

3.4.3 Testing techniques. A common testing technique for comparing bone strength is three-point bending tests. In the three-point bending test, the bone is placed atop two separate points, with a third point atop the bone, situated in between the two bottom points (Fig 17). A load is applied from the top point that is placed onto the bone, until it begins to yield, and ultimately, fracture. Three-point bending can test for a wide variety of mechanical properties, such as stiffness, yield load, maximum load, and the total work required to fracture. Stiffer bones require more force to displace the loading point. Yield load is a measurement of the amount of loading the bone can withstand before it suffers permanent damage, while maximum load indicates the largest amount of force the bone is able to handle before fracturing. Both measurements, in Newtons (N), can be thought of as the strength of the bone, assuming cross-sectional areas are equal. The total work required to fracture, measured generally in Newton-millimeters (N-mm),

is the total work that must be done to cause the bone to fracture. Bones undergoing loss of density and trabeculae are expected to have lower values than normal bones when subjected to three-point bending tests [41].

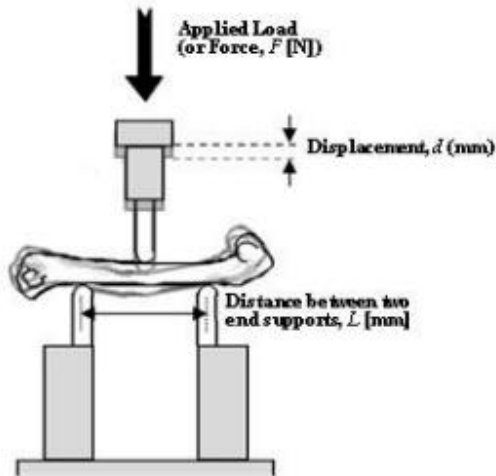


Figure 17. Diagram of standard three-point bending set-up. Bone is placed between two bottom points and top, force applied point [41]

Three point bending studies conducted with healthy human tibias have found varying values in elastic modulus dependent upon the section of the bone being succumbed to a load. Differences in bone type, such as trabecular versus cortical bone, have been found to have different yield strengths. It has been reported that the average yield strength of singular trabeculae, at around 10.4 GPa, is significantly lower than that of cortical bone, at 18.6 GPa [77]. Other studies conducted looking at different areas of the bone have also shown differences in elastic modulus. An average of 14.1 GPa dry, and 11.3 GPa wet, was measured in human medial tibia. In the proximal tibia, values of

10.4 GPa were observed. A study with an entire fresh human tibia found an average elastic modulus of 11.2 GPa [78].

Three point bending with individuals undergone bone degradation, such as those suffering from osteoporosis, can note changes in the mechanical properties of the bone. One study measured the strength of human femoral cortical bone samples undergone three point bending. The bending modulus compared to healthy femur bones was reduced by 22%, and the yield strength by 27% [79]. In another study comparing trabecular bone of osteoporotic individuals who had undergone bone degradation, three point testing was carried out. The Young's modulus was found to be 1.2 GPa compared to 2.16 GPa in healthy boned individuals, along with a yield strength of 0.03 GPa compared to 0.04 GPa, and an ultimate stress of 0.04 GPa to 0.05 GPa. Other variables that were tested during the three-point bending include bending stiffness, work to failure, and fracture load, all of which were lower in the individuals suffering from bone loss (Fig. 18) [80].

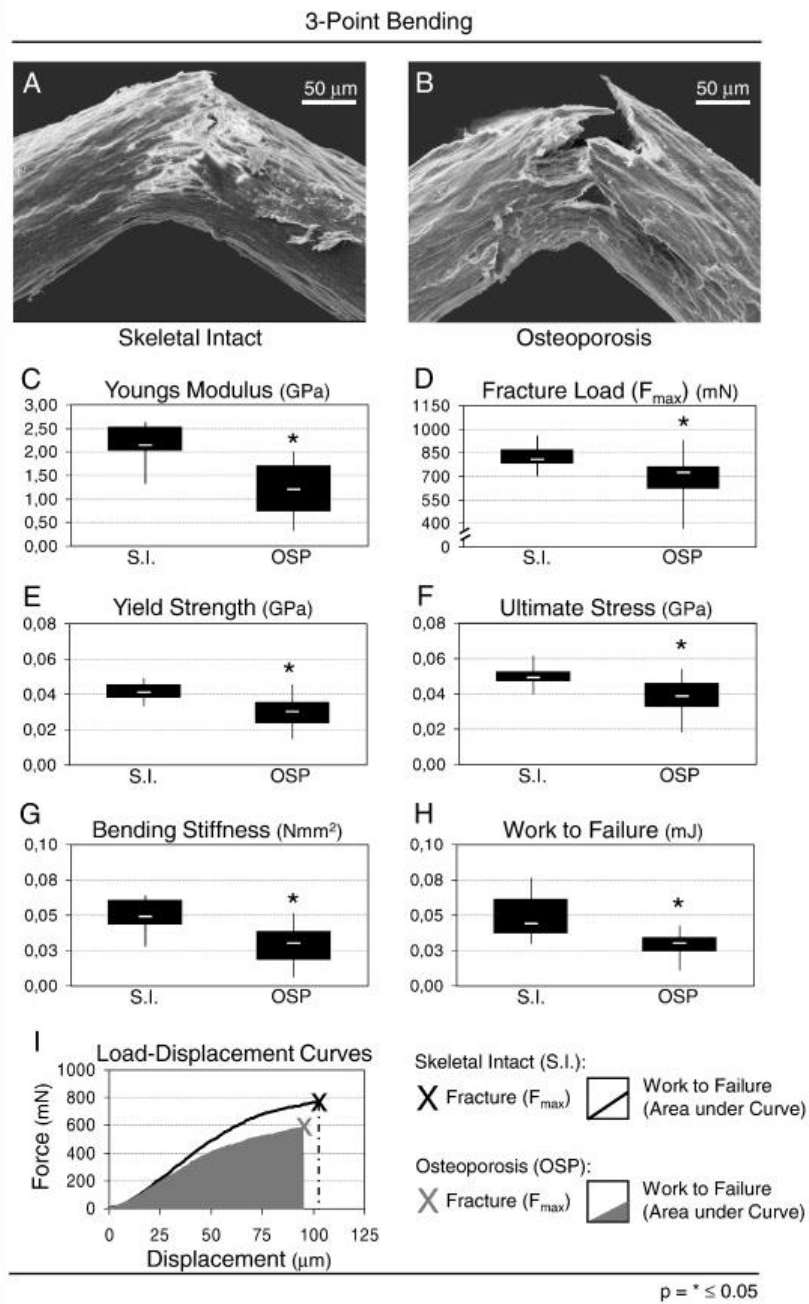


Figure 18. Variables measured from three-Point bending tests conducted on normal (S.I.) and osteoporotic (OSP) trabecular bone [80]

3.5 Animal Studies

3.5.1 Muscle changes. While not as common as human SCI studies, there have been studies in animals that have shown muscle atrophy and degradation following SCI. One study reported in rats with their T10 cord severed, leading to a group of paraplegic rats, the gastrocnemius muscle, when subjected to mechanical load testing at two weeks, found the ultimate load and stiffness were 55.7% and 22.9% lower, and after four weeks the parameters were 62.8% and 29.5% lower, respectively [43].

In another study, changes in mass of the soleus and tibialis anterior muscles that were recorded following SCI in rats at two weeks showed significant reductions; the soleus and tibialis anterior of the control groups weighed in at an average of 0.1232g and 43.1g, respectively, while measurements for the SCI group weighed in at an average of 0.0773g and 30.0g, respectively. This represents a 37.26% reduction in the soleus and a 30.39% reduction in the tibialis anterior. This same study also found that the structure of muscle was altered, with SCI reducing the amount of slow muscle fibers found in both muscles [44].

Another study looked at muscle mass of the soleus in T7—9 SCI contused rats three weeks post-injury. A decrease in mass by 20% compared to control animals was measured. Cross-sectional areas of the gastrocnemius and soleus were found to be only 75% of that of normal animals as soon as one week after injury; this decrease was found to remain relatively stable over time, with other combinational immobilization techniques reducing the mass and cross sectional areas to a greater extent [76].

3.5.2 Bone changes. It has been demonstrated that bone loss, such as a decrease in bone mineral density and biomechanical strength, significantly occurs in the lower limbs as soon as two weeks following SCI in rats [45]. Cancellous bone volume in another rat SCI study displayed a 25% decrease compared to uninjured, normal animals in hind limbs, and losing about 11% of their cortical bone mass within 2 weeks. In the metaphyseal tibial region, the trabecular bone strength was approximately cut in half [46]. Total bone mass of the femur and tibia has shown dramatic decreases as well. In a 63 day study, at day 33 femoral mass in rats had decreased by 16%, to a total of 33% by the final day. Similarly, tibial bone mass decreased by 16% 33 days after SCI, to 34% on day 63 [8].

In another study taking a closer look at the bone microstructure properties with SCI, after 16 weeks, the femoral bones had a 65% reduction in bone volume over tissue volume, a 36% decrease in trabecular number, a 26% decrease in trabecular thickness, and a 73% increase in trabecular separation. Cortical thickness was also decreased by 16% [47]. Another study of tibial rat bone post-SCI showed similar patterns, with a significant decrease seen in bone volume, trabecular number, and trabecular thickness after three weeks. A study by the same group also found similar results for femoral rat bone [48]. All aforementioned animal studies had SCI occur between the T9—10 or T11—12 spinal sites.

3.5.3 Testing techniques. Studies of three-point bending with bones from SCI animals have shown that in rat tibias, following two weeks after SCI, there was a statistically significant decrease in the maximum load that could be put onto the bones before fracture. Bones succumbed to three-point bending four and six weeks post-injury

did not show any more significant changes compared to that of the two week post-injury mark (Fig. 19) [45]. Another study looked at three-point bending after three weeks, six weeks, and six months. The ultimate load of the tibia was reduced as time went on, though the initial three week measurement showed the largest decrease, with the last two being only slightly lower than it. Similar results were seen in the ultimate load of the femur. The normal group saw an ultimate tibial load of 149.2N, and the SCI 62.6N three weeks after injury. Similar results were seen with the femur, with the uninjured taking an ultimate load of 131.5N, and the SCI group 57.4N after three weeks [48].

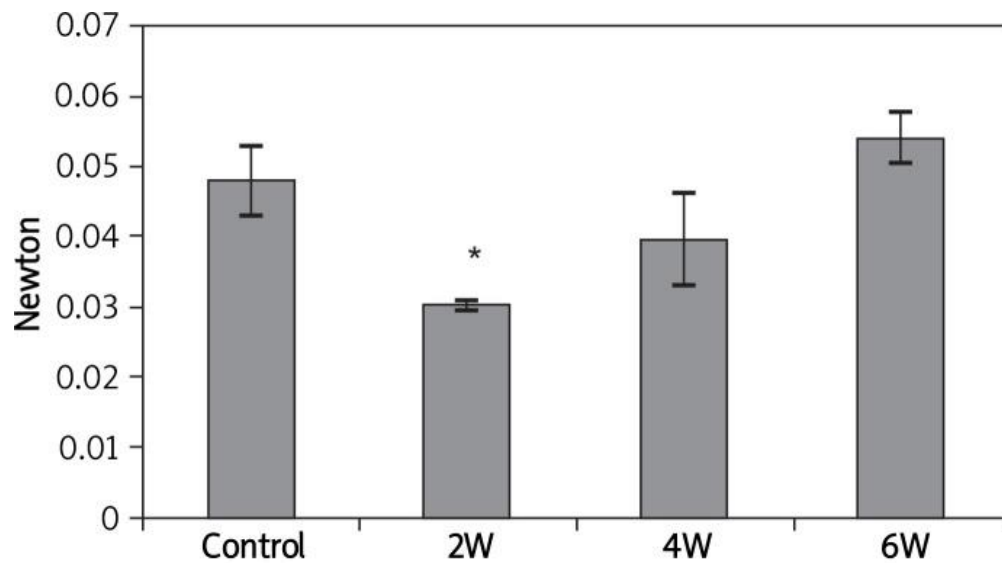


Figure 19. Biomechanical testing via three-point bending on SCI rats two, four and six weeks post injury versus the noninjured control group [45].

3.6 Conclusion

Bone and muscle changes following SCI can be drastically seen. In those suffering from thoracic SCI, the loss of mobility in their lower limbs greatly affects the areas, mass, and mechanical properties of both the bones and muscle. Bone testing techniques, such as three-point bending of SCI individuals have also demonstrated the affects it has compared to normal persons. Overall, muscle area is shown to have a more substantial decrease than bone in the lower limbs, suggesting that muscle atrophy may be higher for SCI persons than bone degradation [33]. Looking at bone properties, it has been noted that cortical bone area does not degrade as significantly as trabecular bone [8]. With the ratio of cortical to trabecular bone higher in the leg bones, it can be expected then that muscle atrophy will be higher than bone. With this point addressed, it is pertinent that appropriate stimulation, via therapy or training, allows proper loading and ambulation such that muscle loss is slowed, but also that there is adequate dynamic movement to slow bone degradation, since there is not necessarily a direct correlation between the amount of muscle atrophy and bone loss [33].

Chapter 4

Current Rehabilitation Strategies to Restore Bone Loss after Spinal Cord Injury

4.1 Introduction

Following SCI, it can be difficult for individuals to get proper rehabilitation treatment. Rehabilitation is important in keeping muscles from undergoing atrophy, and bones from undergoing loss and resorption. As mentioned in Chapter 3, some sort of stimulus, mechanical for bone movement and a loading force for muscle, is necessary to keep such loss at a minimum, or to even prevent it entirely. Since bone loss and muscle atrophy does not occur at the same rates, different rehabilitation strategies have been implemented to attempt and restore both. Passive training and active training are two common strategies, with passive requiring little to no effort on the individual, and active requiring some type of exertion of the individual. Training is a necessary step on the path to some functional and anatomical recovery, and helps in reducing problems that come from inactivity, such as osteoporosis and cardiovascular diseases.

4.2 Passive Training

When a patient is undergoing passive training, they are not in control or in charge of their movements. A machine or trainer provides the force and exertion to move the trainees' limbs to try and work the muscle (Figs. 20, 21). Most common passive techniques include some sort of range of motion (ROM) exercise, helping to stretch the muscle and joints. Motorized bikes or robotic assisted devices are two commonly seen passive training techniques. Passive training is commonly seen in individuals suffering from a range of paralysis, such as SCI or stroke patients. ROM exercises can help stiff

and spastic muscles, or muscles that have limited control, coordination, and movement. A benefit of passive training is that it can be initiated at earlier stages in the recovery process than active training [3].



Figure 20. Example of a passive training device meant to stretch the radiocarpal (wrist) joint [49]

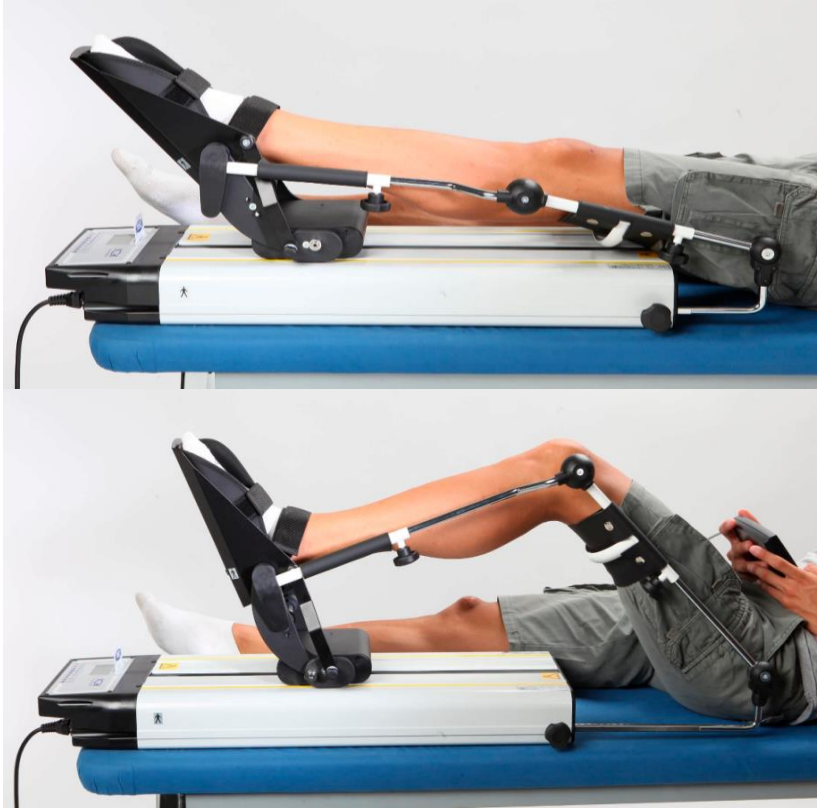


Figure 21. Example of passive training device meant to stretch hip, knee, and ankle joints [50]

Stretching of the muscle and moving the joints has been shown to activate the Hoffman-reflex (H-reflex) of specific muscle spindles, utilizing synergistic muscles only, and no antagonistic muscles. The H-reflex is a reaction of the muscle caused by the electrical stimulation of afferents that originate in the muscles' spindles. Through repetitive passive training, continual activation of the H-reflex can better train the caudal circuitry in the spine to hone in on spinal reflexes which are often absent following SCI. Decreased spasticity can be seen, although training needs to be continued and not stopped to see recovery maintained [3].

4.3 Active Training

Unlike passive training, active training requires the trainee to exert their own force to move their muscles and joints. While active training can include ROM and stretching exercises so long as the person is doing it unaided, it also includes active loading, or weight bearing exercises. This helps strengthen muscle and bone, and can also help improve neural pathways as one continues to perform the training routinely. Locomotor training, such as manual or robot assisted treadmill training, is a commonly used technique (Fig. 22). Locomotor training is a popular technique for incomplete SCI patients, with improvements generally seen in mobility. Locomotion along with body weight supported treadmill training (BWSTT), a similar training method, can start as early as four weeks after the injury. A harness is utilized to suspend the patient, with manual assistance needed if no movement is yet seen in the lower limbs. Moving the patients legs are essential in creating a patterned movement, creating a muscle activation process that aids in recovery [4].

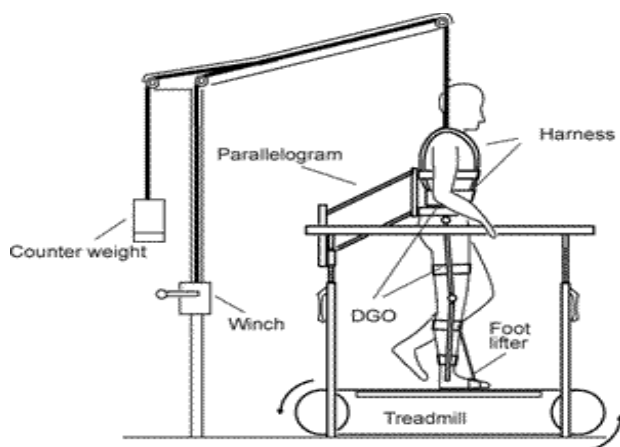


Figure 22. Schematic of body weight supported treadmill for active training [4]

Specifically, active training has been seen to decrease the role of any inhibitory factors in muscles, while increasing neurotrophic factors that support the growth and development of neurons [4]. Brain derived neurotrophic factors (BDNF) is a potential key player in the axonal growth, and has been found in higher levels of exercised subjects. Neuroplasticity, growth and recovery all appear to coincide with BDNF expression; rewiring of the motor cortex can be another possible advantage of active training, allowing signals to find new pathways instead of travelling along broken pathways left over from SCI [4].

4.4 Human Studies

4.4.1 Passive training. In a study following 31 patients with complete SCI, passive rehabilitation therapies were utilized through passive standing and loading. Paraplegics using standing frames or braces had significantly higher lower limb bone area, though muscle area showed no significant difference [33]. Looking only at muscle area changes, another study compared the effects of limited mobility (wheelchair confinement) to that of passive standing on subjects with incomplete SCI. Results found that muscle atrophy was significantly greater, with a maximum difference of 39% occurring in the gastrocnemius muscles [51]. Another study with passive cycling was observed in SCI patients trained for 30 min/day, 3 days/week for one year. The initial measurements of proximal tibial density averaged at 52% of that of a normal person. After one year of training, density increased by 10% [52]. A different study combined cycling with functional electrical stimulation (FES) initially for three months with four sessions per week, one hour each, before increasing to five times a week (Fig. 23). Femur density increased by 7%, while no change was seen in the tibial bone. It had been noted

that the femur, from the FES placement, had similarities of active training from muscle contraction in the thigh, while the lower leg followed a more passive training routine. Muscle of the thigh increased in cross sectional area by 34.4%, though no significant changes were seen in the lower leg [53].



Figure 23. Passive cycling set-up with FES of hind limb training [53]

4.4.2 Active training. A study of five individuals succumbed to BWSTT 2—6 months following SCI was conducted. The injured were fitted via a harness and a level of weight chosen so that each person could properly stay erect without their knees buckling. Walking time, beginning at five minutes and eventually reaching 15 minutes, along with a treadmill speed of no more than 0.6km/h were two main facets of the training paradigm that lasted 48 sessions. Following scans and analysis, it was found that bone mineral density did decrease at a range from 4.3—22.6%. There seemed to be a connection between how much bone density was lost, and how little advancements one made in

walking, i.e., the individual who was not able to complete the training had the largest decrease. While this study did not correlate BWSTT with halting bone loss, it did appear to minimize the effects compared to if no training was undergone. However, all individuals did have an increase in muscle area of the thigh and calf muscle post-training. At the start of training, the injured persons had a muscle area about 60—65% of that of an uninjured person. After 48 sessions, the muscle area increased to 72—79% of that of normal persons [54].

A similar study of 14 SCI participants at least one year post-injury followed a BWSTT regiment of 144 training sessions. No significant changes in bone density were seen, although there also appeared to be no apparent decrease. Muscle area analysis displayed an increase in 4.9—8.2% in thigh and lower leg muscle from the start of training [55].

4.5 Animal Studies

4.5.1 Passive training. Rats given a laminectomy at the T10 level underwent a training regimen of passive standing, being held up by a standing frame that extended the animals' hind limbs. Tibia and femur bones were scanned and analyzed, to compare to uninjured rats, rats with SCI and no training, and those with SCI that underwent passive training. Rats with SCI and no training saw a 31% reduction in femoral mass after 33 days, and a 33% reduction after 63 days. When passive standing was started as soon as three days after SCI for short-term training, the rats in that group had increased their femoral mass by 9%; when training was conducted throughout the length of the experiment, a femoral mass increase of 36% was found. It was of interest to see if similar

patterns were found with the tibial bone mass. After 33 days, a 16% decrease in mass was found, which decreased to 34% after 63 days in the injury only group. Passive standing as a long term treatment actually was found to increase tibial mass by 46%. Short term training did not appear to have any significant effects to tibial mass. The mechanical load that was placed on the rats hind limbs while standing appeared to improve the bone microstructure. Electrical stimulation was also another test, but results did not prove to be as significant in improving bone or tissue lost (Fig. 24) [8].

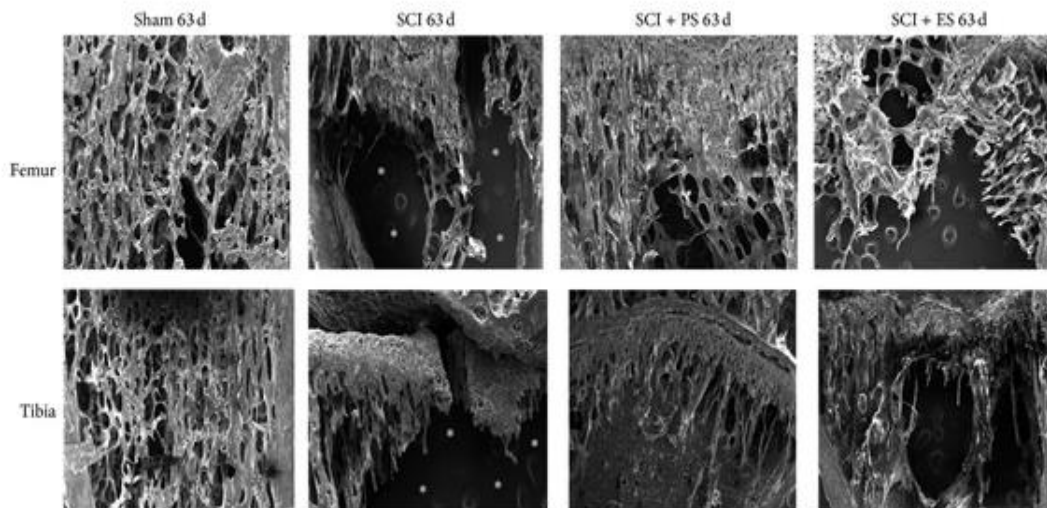


Figure 24. Scanned electron microscopy (SEM) images of the femur (top) and tibia (bottom) of normal rats, SCI rats, SCI with passive standing (PS) rats, and SCI with electrical stimulation (ES) rats after 63 days. Large spaces where bone resorption has occurred can be seen in SCI and SCI+ES rats, whereas SCI+PS has less bone loss [8]

Another study comparing the effects of a 21-day passive versus active stepping paradigm on a built stepper device was employed on rats. At the end of the study, the passively trained animals showed lower trabecular bone mineral density compared to the active trained group, along with lower tibial values in trabecular thickness, trabecular

number, and a slight increase in trabecular separation compared to the active steppers. Calf muscle area was lower in passively trained groups versus actively trained groups. However, tibia bone microstructure values from passively trained rats were still higher in bone volume over tissue volume, trabecular thickness, trabecular number, and lower in trabecular separation than the untrained rats [81].

Three point bending conducted with passively stepping-trained rats after a 21-day program displayed higher stiffness, maximum load, energy absorption, and Young's modulus versus the non-passively trained, though none of the values were significantly greater. Rats trained with a more active stepping paradigm did show significant differences to untrained rats in maximum load, stiffness, energy absorption and Young's modulus [81].

4.5.2 Active training. Treadmill training of 30 minutes or 60 minutes, five days a week, for 13 weeks was compared in rats to see any changes in bone mineral density. Scans conducted showed that the longer exposure to mechanical stress correlated to a greater increase in tibial density, with the hour long trained group having higher density values [56]. A similar study focusing on the bone microstructure properties of the trabeculae in treadmill trained rats, trained for 10 weeks for 60 minutes, scanned the hind tibias and femurs via micro-CT. Bone mineral density of the femur was significantly higher in trained groups than controlled. Looking at the femoral trabecular properties, bone volume over total volume, trabecular thickness, and trabecular number were are significantly higher in the treadmill trained group; trabecular separation was also seen to be significantly lower. No significant changes in calf muscle mass were seen [57].

The same study also conducted three-point bending tests on the femurs of both trained and non-trained groups. For the trained set, maximum load and stiffness values, especially of the mid-femur, were significantly greater [57].

Jumping exercises have been employed as another type of active training method. Rats were placed in a height-adjustable box where electrical stimuli initially forced rats to jump, with the stimulus becoming used less as rats became accustomed to the procedure. Ten jumps a day were carried out five days/week for five weeks total. The height of the box was increased from 25cm to 40cm. The bone mineral density of the femur was significantly higher in all regions in the jump group versus the control. Looking at the bone microstructure, the jump group also had a 31% increase in trabecular number, and a 63% increase in trabecular thickness [58].

4.6 Goal

Beginning at the onset of any debilitating injury limiting or halting movement, the bones and muscles of the immobile limbs begin to deteriorate and atrophy. As discussed in Chapter 3, bone loss and muscle atrophy, while occurring at different rates, are most apparently seen in the hind limbs. Following a SCI at the T11—12 level for example, the most common thoracic spinal injury, the lower limbs may experience varying loss of function [17]. Keeping one immobile and allowing bone density and muscle area to decline can lead to osteoporosis and numerous other diseases, along with metabolic function decrease. However, many patients can recover partial sensations and movement through training paradigms. At this point, passive and active training are two most common techniques in attempting to restore any bone and muscle loss resulting

from injury. While both can be implemented depending on how recent the injury was, it is important to better understand how the methods can better promote regeneration and growth. While studies have been done on humans and animals covering active or passive training, an important goal would be in comparing the two methods directly in a single experimental study. The next chapter is the scientific paper of this thesis, aiming to compare the effects passive and active training has comparatively on bone microstructure properties and recovery following thoracic spinal cord injury in rats.

Chapter 5

Effects of Training Paradigms on Bone Recovery after Spinal Cord Injury in Animals

B. King¹, J. Witko¹, J. Kadlowec¹, A. Singh²

(1) Mechanical Engineering Department, Rowan University, Glassboro NJ, USA

(2) Biomedical Engineering Department, Widener University, Chester PA, USA

5.1 Abstract

The effects spinal cord injury (SCI) has have been studied in both human and animal models. Specifically in incomplete SCI, the bone degradation and muscle atrophy seen in the lower limbs has been documented, along with the effects of different training paradigms on bone and muscle loss. This study implemented a clinically relevant animal model of a moderate spinal contusion injury at the T9—T10 level, along with active body weight supported treadmill training (BWSTT) and passive bike training, to compare the effects such training methods have on the bone microstructure properties and muscle masses in the lower limbs of rats. Behavioral BBB and wire grid testing, along with three-point bending, was conducted. Our results showed that both passive and active trained animals did not show any significant differences from normal animals in metaphyseal region bone volume over total volume (BV/TV), and bike trained animals had no significant differences in trabecular separation (Tb.Sp) from normal animals. Further comparisons were drawn from the remaining properties of trabecular thickness

(Tb.Th), trabecular number (Tb.N), and soleus muscle masses. This study allows for a comprehensive view of bone recovery on SCI with active and passive training paradigms.

5.2 Introduction

Spinal cord injury (SCI) affects 54 million individuals in the U.S., with an additional 17,000 cases added in the year 2016 alone [1]. The most common causes of SCI include vehicular accidents, falls, acts of violence, and sports related injuries. SCI cases include both incomplete, where neurological pathways at the injury site are spared, and complete, where pathways at the injury site are not spared. Tetraplegia and paraplegia refer to if paralysis occurs throughout the entire body, or lower half of the body, respectively [1]. Due to the debilitating nature of SCI, it is important that effective training takes place as soon as possible following injury.

Primary and secondary damage following SCI cause negative changes to both the spine and the body, especially that below which the injury has occurred. Primary damage includes contusions, cell death, and axon death. Secondary damage includes ischemia, hypoxia, infections, as well as degradation and atrophy to the limbs below the injury [16]. While not much can be done to avoid primary damage, training can help halt some secondary damage. This is especially true for bone degradation and muscle atrophy.

Decreases in muscle mass are commonly seen in both human and animal SCI models, along with loss of bone density that can be characterized by its microarchitectural or microstructure properties of both the cortical and trabecular bone. These include the bone volume over the total volume (BV/TV%), the trabecular thickness (Tb.Th), the trabecular separation (Tb.Sp), and trabecular number (Tb.N). Common

training techniques include passive training, which allows the trainee to perform stretching and range of motion (ROM) routines without any direct control over their movements, and active training, which requires the trainee to exert their own force to mobilize their muscles and joints [3,4]. Both have been studied in human and animal models to see the effects the training paradigms have on limbs below SCI sites. This study will focus on both active and passive training in a clinically relevant thoracic SCI animal model to compare the effects they have on bone and muscle properties

5.2.1 Current aim. The current aim of this study is to investigate the effects that active, body weight supported treadmill training (BWSTT), and passive bike training have on muscle mass and bone microstructural properties following a T9—10 level contusion injury in a clinically relevant SCI animal model.

5.3 Methods & Materials

5.3.1 Spinal cord injury. All described animal surgeries, care, and protocols were in accordance with the National Institute of Health (NIH) *Guide for the Care and Use of Laboratory Animals*, with approval granted by the Rowan University School of Osteopathic Medicine Institutional Animal Care and Use Committee (IACUC). A total of 30 adult female Sprague-Dawley rats (225-250g, Harlen NJ) were used in this study. They were initially housed in groups of 2—3 per cage until surgery with alpha-dry bedding and free access to food and water on a 12-hour light and dark cycle. Animals were broken down into four groups, depending on injury and training method of active body weight supported treadmill training (BWSTT) or passive bike training, as seen in Table 2.

Table 2

Number of Animals in each group

Group Number	Description	Number of Animals
Group 1	Normal	7
Group 2	Contused SCI	8
Group 3	Contused SCI + BWSTT	8
Group 4	Contused SCI + Bike	7

Groups 2—4 were prepared for spinal surgery by giving an anesthesia cocktail injection of ketamine (76mg/kg, Fort Dodge Animal Health, Fort Dodge IA), xylazine (7.6mg/kg, Ben Venue Laboratories, Bedford OH), and acepromazine maleate (0.6mg/kg, Boehringer Ingelheim Vetmedica INC, St. Joseph MO). The animals were prepped for surgery by having their backs shaved and cleaned with alcohol and betadine. A T9—10 laminectomy was performed to expose the dura, and a moderate contusion injury was given via an impactor device (Impactor Model-II, W.M. Keck Center for Collaborative Neuroscience, Rutgers University NJ) with a 10g, 2.0mm diameter rod dropped from 25mm above the T9—10 cord. A piece of subcutaneous fat was laid over the exposed dura to prevent any adhesions. The back muscles were closed with 4.0 sutures, and the skin with surgical wound clips. Rats were left individually in new, clean cages with heating pads until they regained consciousness and were able to move. Long-stemmed water bottles were used to better enable the rats to get water, along with H₂O hydrogels and food placed directly in the cage.

5.3.2 Animal care. Following surgery, all rats were injected subcutaneously with 3—5ml of saline two times a day, about 10—12 hours apart, and ampicillin (0.1cc, 22.7mg/ml) once a day for 14 days. Bladders were manually expressed three times a day, with urine tests conducted via urine test strips (Henry Schein Urispec 11-Way Reagent Strips) to monitor for abnormal protein, nitrite, ketone, glucose, and leucocyte levels. Bladder results were recorded, along with checking off administered injections in a daily log. All injections and bladder tests were performed for two weeks post-surgery to help prevent risk of dehydration and infection. If signs of illness were present, rats were given 0.4ml (100mg/kg) of Children’s Tylenol orally once a day as needed. Rat cages were changed twice a week, along with new water, cardboard tubes, food, and bedding given.

5.3.3 Behavioral Analysis.

5.3.3.1 BBB testing. Following the Basso, Beattie and Bresnahan protocol [72], all rats were placed in a circular enclosure and video recorded for 4 minutes by an observer. The BBB tests were first conducted before the SCI for a baseline measurement, followed by 2—3 days after surgery, and each week after until the 9th week. Rats were then scored by a blind observer based on their neurological rating, given a score of 0 (complete hindlimb paralysis) to 21 (normal hindlimb locomotion).

5.3.3.2 Wire grid testing. All animals were placed atop of a metal grid about 18 inches off the ground and made to navigate around the grid (Fig 25). Animals were recorded for two minutes by an observer. A mirror was placed behind the animals and grid, opposite to the camera to get an unhindered, alternate view of the rats’ motor coordination. Any slipping of the hind limbs was recorded. This test was conducted prior

to SCI and at week 8 post-injury to injury only, BWSTT, and Bike groups. A blind observer recorded the number of total steps to missteps.



Figure 25. Wire Grid behavioral analysis set up

5.3.4 Treadmill training. BWSTT started one week post-surgery. All treadmill training animals were secured to a body weight support arm via Velcro and a soft vest to a custom built treadmill (Fig. 26). A load cell was attached to the body weight support arm to measure the load the rat exerted when walking. Rats were trained at 75% of their body weight support at a speed of 7cm/s. A total of 1000 steps a day were performed for each rat, 5 days/week for 8 weeks. A trainer held the rat's upper foot and helped guide their 1000 steps (Fig. 27).



Figure 26. Images of the custom built body weight support treadmill. (A) National Instruments myDAQ system, paired with LabVIEW VI operating system; (B) Treadmill motor controller connected to myDAQ, controlling motor to drive treadmill; (C) Tensioning motor controller connected to myDAQ, controlling tension in spring; (D) Power supply cord, connects to outlet; (E) Treadmill motor; (F) Adjustment knob to lower or raise body weight support arm; (G) Animal attachment plate; (H) Load cell, measuring weight animal is subjected to; (I) Load cell amplification circuit, amplifying load cell signal before processed by myDAQ; (J) Tension spring, proving assistance to animal; (K) Spring tension motor, changes tension of spring via tension motor controller; (L) Treadmill belt; (M) Base of treadmill; (N) Body weight support carriage, attached to the adjustment knob and moves spring and load cell



Figure 27. Trainer with rat, demonstrating BWSTT

5.3.5 Bike training. Bike training started one week post-surgery. All bike animals were secured to a soft base via medical wrap bandages, with their hind feet attached to the paddles via medical skin tape. A motor powered all the bikes, which were connected to each other so that they'd turn simultaneously and together (Fig. 28). Animals were trained for a total of 40 minutes, with 20 minutes of training followed by a rest period and an additional 20 minutes of training at 45 rpm. The training occurred 5 days/week for 8 weeks.



Figure 28: Image of bike set up. (A) Rectangular frame for holding rat, screwed into place by adjustable knobs attached to vertical metal rods; (B) Base frame, supporting rotating connectors and pedals; (C) Base connectors held in place by metal screws; (D) DC Motor with adjustable speed control, powers pedals

5.3.6 Animal sacrifice. Following the conclusion of all animal training and behavioral analysis testing, animals were sacrificed by being given a 1.0 ml injection of Euthasol (Virbac AH, Fort Worth, TX). Once animals were sacrificed, the soleus muscle was extracted from each rat hind limb, and weighed, along with the hind tibia bones of each rat hind limb extracted. Bones were immediately stored in a freezer until analysis.

5.3.7 Bone analysis.

5.3.7.1 X-Ray & Micro-CT. All hind bones were harvested and stored in a freezer following animal sacrifice. To begin the x-ray imaging, tibia bones were removed from the freezer and weighed. The bones were then wrapped in para-film and wetted with saline. The wrapped bones were placed in a tube with para-film covering both ends. A brass stage was utilized to give a proper height for the bone, placed vertically with the metaphysis end pointing down (Fig 29). The resolution was conducted at $4.9\mu\text{m}$, the camera at medium pixel size of 2000×1000 , and the filter AL 0.5mm. Voltage was 65kV, and current $156\mu\text{A}$. Both the metaphyseal and diaphyseal regions were scanned (Fig 30). The metaphyseal region scan began at the growth plate to a distance of 3mm below, and the diaphyseal region was scanned 1.5mm above to 1.5mm below the center of the tibia bone. SkyScan Micro-CT X-Ray machine and its corresponding software were used.



Figure 29. Rat tibia in para-film wrapped tube on top of metal brass stage prepared for scanning

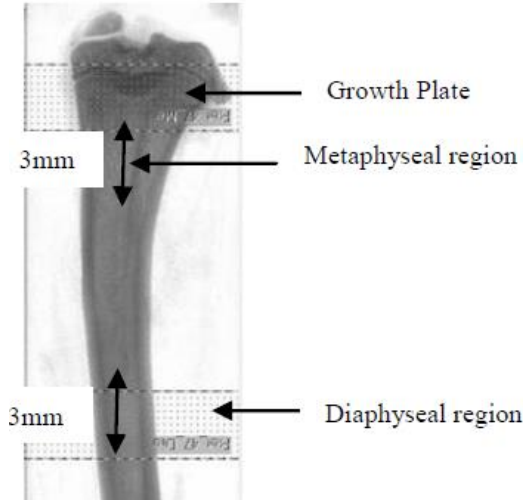


Figure 30. Longitudinal image of rat tibia metaphysis (top) & diaphysis (bottom) regions scanned

Once scanning was finished, reconstruction was performed via the NRecon program. A misalignment compensation of 1.5, a ring artifacts reduction of 10, and beam-hardening correction of 40% were used.

Analysis was conducted with the CTan program following the scanning and reconstruction of the metaphyseal and diaphyseal bone sections. For the metaphysis, both cortical and trabecular bone were accounted for. Thresholding, despeckling, region of interest shrink wrapping, 2D analysis and 3D analysis were performed. Properties studied were: bone volume over total volume (BV/TV), trabecular thickness (Tb.Th), trabecular separation (Tb.Sp), and trabecular number (Tb.N). 3D reconstruction was also undertaken through CTan, with the CTvol program working in conjunction to process and open the trabecular images.

5.3.7.2 Three-Point bending. Rat tibia bones were isolated from the animal after sacrifice and wrapped in saline wetted gauze for storage in a freezer until the three-point bending tests could be conducted. Tibias were taken out of the wrapping and placed atop the two bottom base points in the mediolateral direction, with the center, diaphysis region of the femur aligned with the top point. A three-point bending test was then performed using ADMET material testing machine (ADMET INC, Norwood MA) until fracture occurred. Load displacement was obtained at a sampling rate of 100 samples/sec, displacement rate of 5 mm/min, with ultimate load obtained for data analysis (Fig 31)

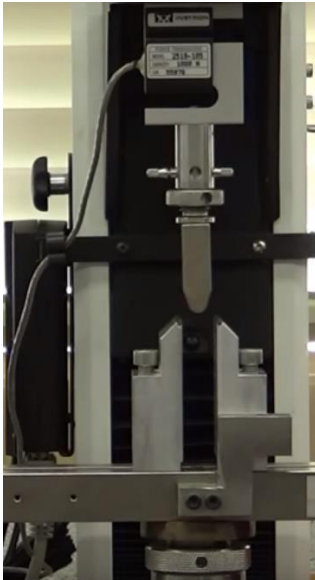


Figure 31. Three-point bending device set up

5.3.8 Muscle mass. Rat soleus muscles were isolated from the animal after sacrifice and weighed. Masses of the muscles were recorded and calculated as % body-weight.

5.4 Results

5.4.1 Behavioral analysis. Weekly BBB scores, including a baseline 2—3 days following injury, can be seen in Fig. 32. Functional recovery can be initially seen in BWSTT and Bike groups, though these values were not statistically significant from the injury group and significantly different from normal.

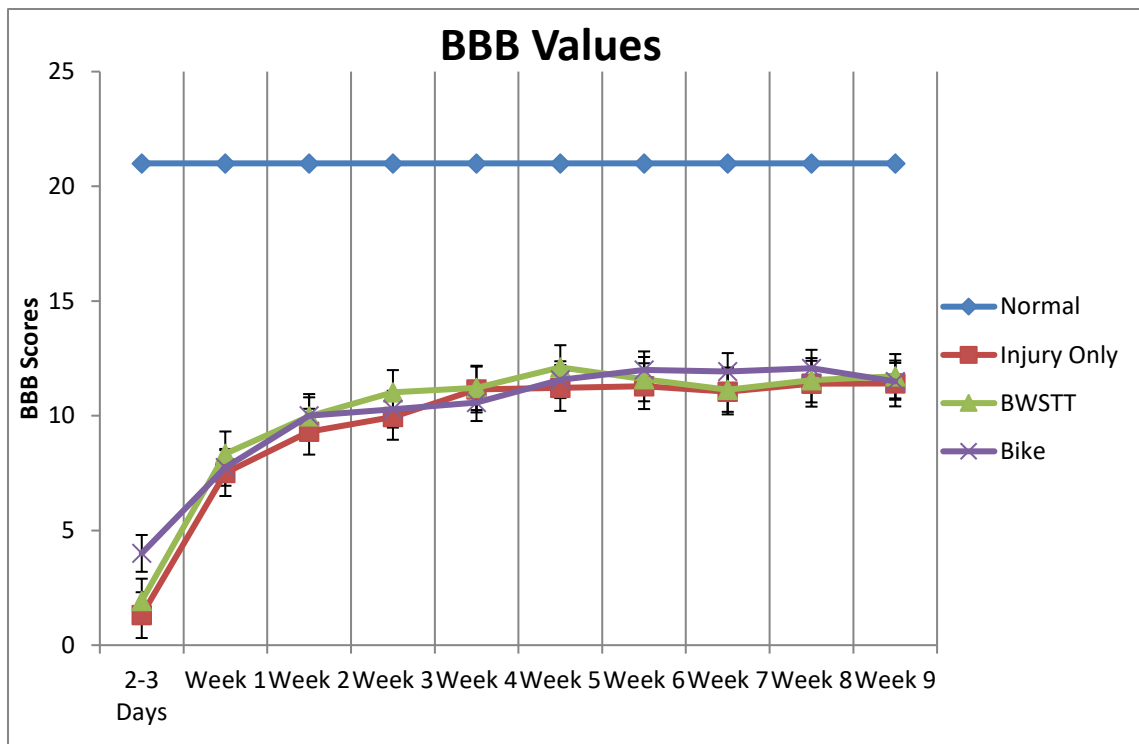


Figure 32. Graph of baseline and weekly BBB scores for rat groups

Grid test scores for normal baseline and Week 8 BWSTT and Bike groups can be seen in Fig 33. Uninjured animals had the highest percentage of normal steps compared to missteps and the injury only, BWSTT and Bike groups had lower percentages of normal steps to missteps. However, there were no significant differences between the three SCI groups. The wire grid results for the normal group were significantly different than those of the three SCI groups.

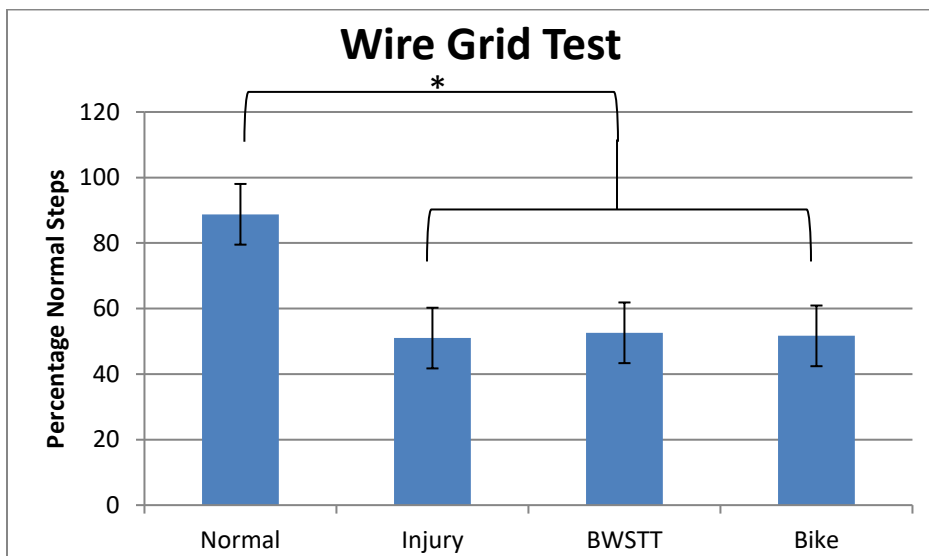


Figure 33. Graph of wire grid testing of differences in normal stepping to missteps in uninjured animals, and injury only, BWSTT, and Bike groups 8 weeks post-SCI.

5.4.2 Bone analysis. The bone volume over total volume was calculated for both the diaphyseal and metaphyseal regions of the rat tibia bone. Fig 34 (a) shows the results of the BV/TV for injury, BWSTT, and Bike groups as a percentage of the normal, uninjured animals' BV/TV. While the diaphyseal regions proved not to show any significant reductions for the injury, BWSTT, and Bike groups, the injury only group

reported a significant reduction in metaphyseal BV/TV compared to normal animals, when the BWSTT and Bike groups did not. Three-dimensional reconstructions of the trabecular regions of each of the four groups of animals can be seen in Fig 35, better visualizing the bone volume kept or lost in each group compared to the normal (Fig 35 (a)).

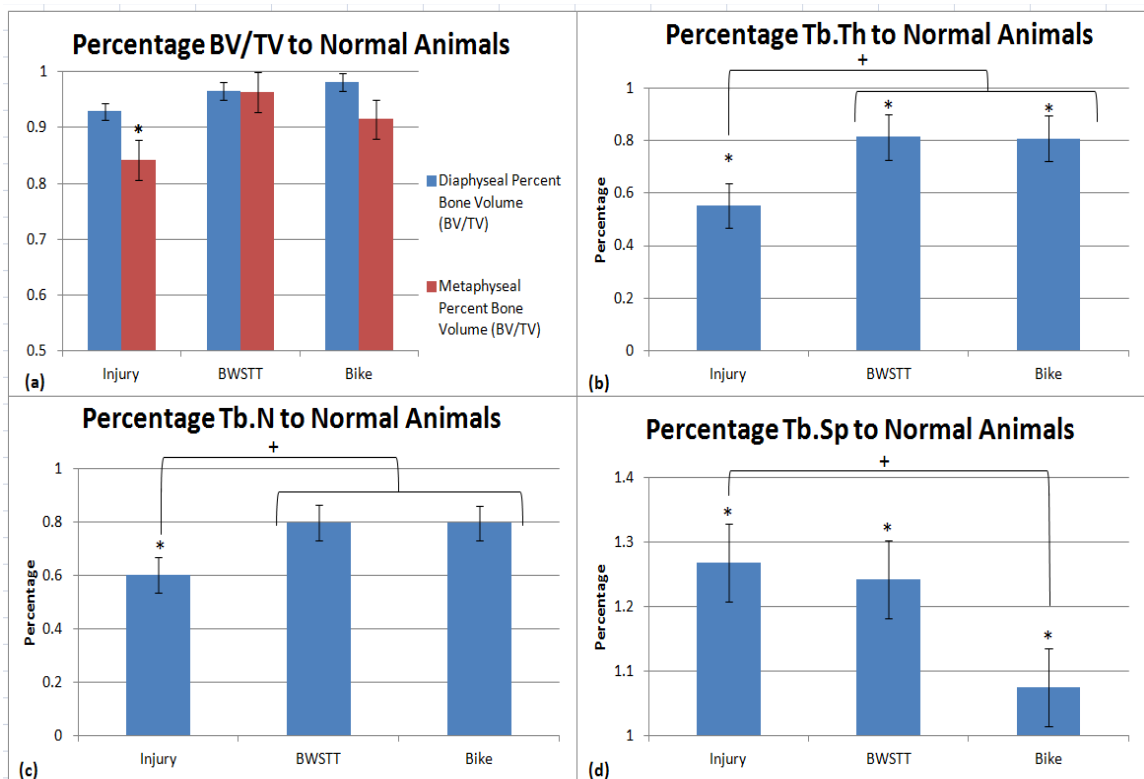


Figure 34. (a) Percentage to normal rats of diaphyseal and metaphyseal BV/TV in SCI rats; (b) Percentage to normal rats of Tb.Th in SCI rats; (c) Percentage to normal rats of Tb.N in SCI rats; (d) Percentage to normal rats of Tb.Sp in SCI rats. (*) = significant difference from normal; (+) = significant difference from trained

Trabecular thickness was measured as the percentage compared to that of normal animals. As seen in Fig 34 (b), injury, BWSTT, and Bike groups all had Tb.Th

percentages that were significantly lower when compared to that of normal animals, along with injured animals being significantly lower than trained animals. Trabecular number was also recorded as a percentage to that of the normal animals (Fig 34 (c)). Injury only rats showed significant decreases to the Tb.N of normal animals, along with being significantly less than Bike animals and BWSTT animals. BWSTT and Bike animals showed no significant differences in Tb.N to normal animals. The trabecular separation percentages of the SCI groups to that of normal animals can be seen in Fig 34 (d). All SCI groups had values significantly greater than normal animals, with injury groups also being significantly greater than Bike animals.

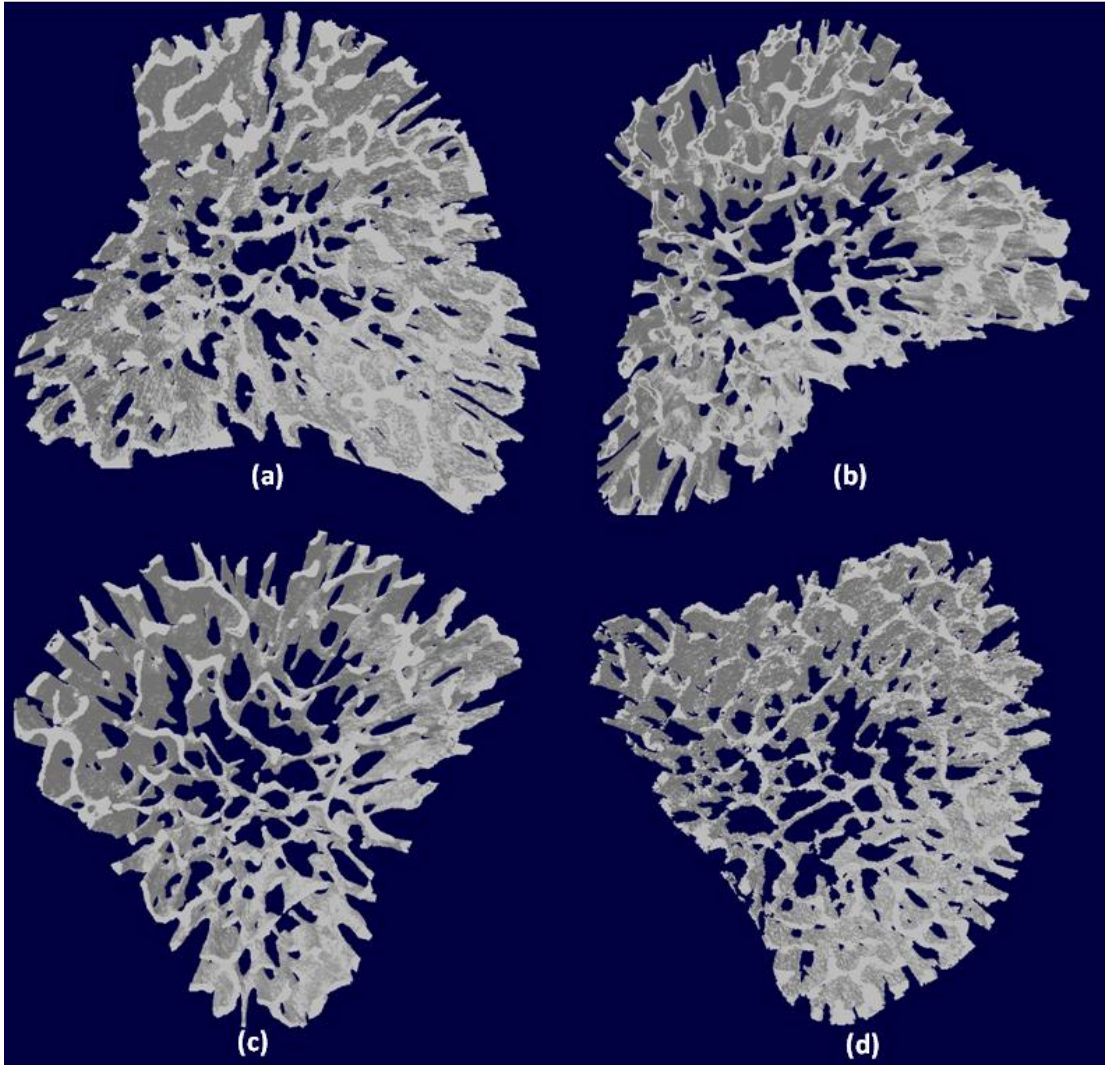


Figure 35. 3D Reconstruction of trabecular bone from (a) normal; (b) injury; (c) BWSTT and (d) Bike rats

5.4.3 Three-Point bending. The results from the three-point bending tests can be seen in Fig. 36. Normal animals demonstrated being able to withstand the largest average load until bending fracture, followed by BWSTT. Bike animals showed similar averages to injury only animals. However, none of the groups were significantly different from each other.

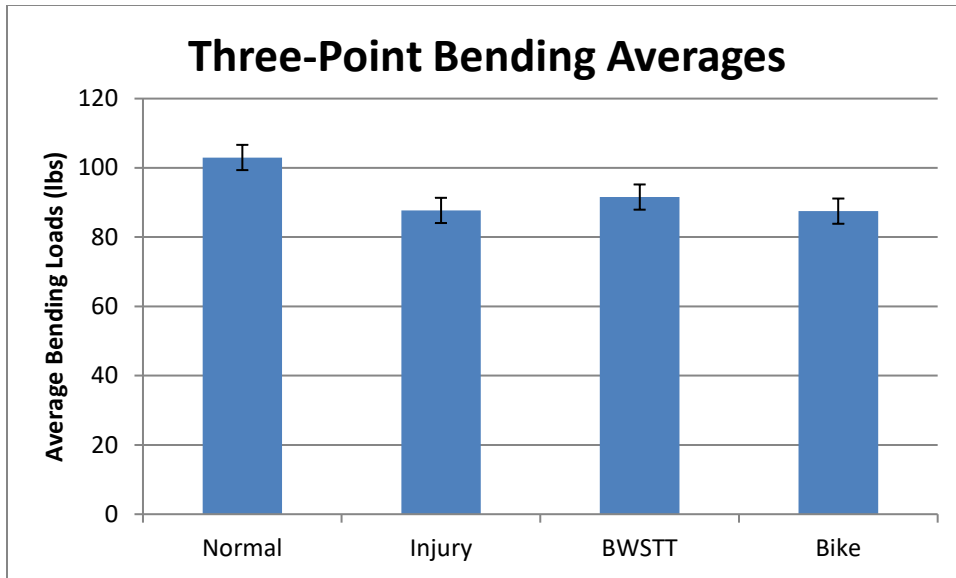


Figure 36. Three-point bending results for normal, injury, BWSTT and Bike rats for average loads until bending

5.4.4 Muscle mass. The soleus muscles of all rats were taken as a percentage of the total weight of the rat. As seen in Fig 37, all SCI groups showed a decrease soleus muscle mass in comparison to normal, uninjured animals. However, the injury only group was the only set where the soleus mass was significantly less, with the BWSTT and Bike groups showing no significant decrease from the normal animals.

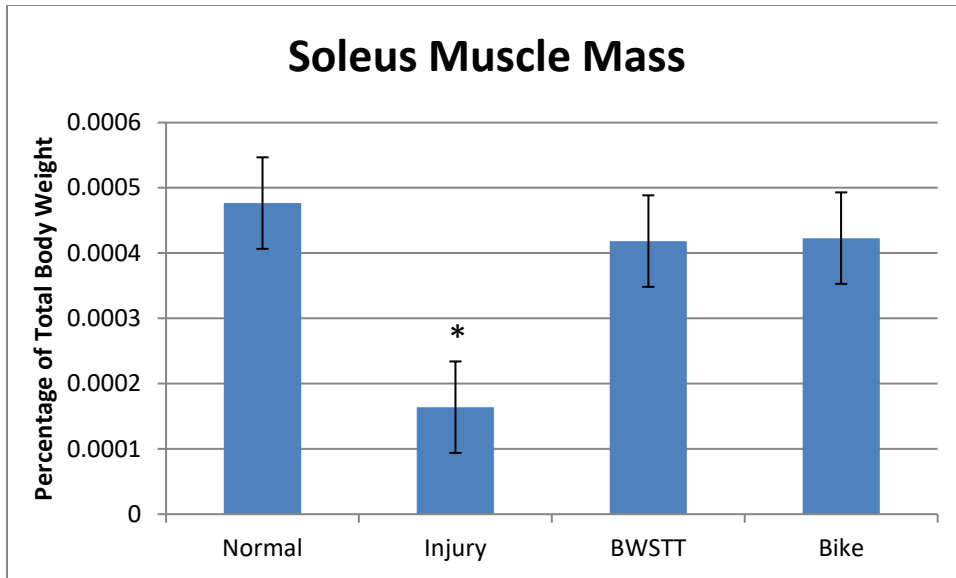


Figure 37. Soleus muscle mass as its percentage to total rat body weight for normal, injury, BWSTT and Bike rats

5.5 Discussion

The contusion model for injury was utilized as it is amongst the better ways, along with compression and hemi-section injuries, to simulate incomplete SCI [24]. Other methods of SCI in animals, such computer controlled injuries utilizing machinery to administer an equal weight to the subject, removes any human differential, but is quite expensive; compression induced injury is another such method that could be employed when looking at lower limbs post-SCI, but the injury does not replicate those seen in humans as similarly as the contusion model does; chemically induced spinal injuries, from injecting excitotoxins into the cord, is better used when studying the underlying mechanisms of the injury itself, and its effect on the spinal column [24].

The behavior analysis BBB and wire grid tests showed no significant differences between the injury only and trained groups following SCI. While these tests can be a common measurement in behavior recovery, they do not give a report of the animals' ability of weight support, or any bone and muscle recovery. Other tests used in this study better represent the bone and muscle recovery of the lower limbs.

The tibia diaphysis and metaphysis regions are comprised of different amounts of cortical and trabecular bone. The diaphysis region, located in the central shaft of the tibia, is made up of almost all cortical bone, while the metaphysis region, located at the medial compartment of the proximal tibia, is comprised of more trabecular bone, surrounded by cortical [10]. These differences in composition can change how the bones react to inactivity or reduced to no usage following SCI, since trabecular bone degrades at a much higher rate than seen in cortical bone [8]. The increased vasculature network seen in trabecular bone enables the increased porosity and softness that is associated with it, but also makes it more susceptible to bone resorption [83]. With the diaphyseal region consisting of no trabecular bone, and the metaphyseal consisting of higher levels, these differences should be reflected in the amount of bone volume over total volume that is lost following SCI. Our results comparing the BV/TV of the diaphyseal regions show that no significant changes in the percentage lost compared to normal animals can be seen, coinciding with the lack of trabecular bone in the diaphyseal region to degenerate. For the metaphyseal regions, injured animals saw significantly reduced BV/TV of 84% to that of normal animals, relating to the greater proportions of trabecular bone known to degenerate following inactivity. This aligns with past studies looking at trabecular bone volume after SCI in rats [8,45,46].

Other bone microstructural properties of injured animals that can be studied looking at trabecular bone include the thickness, separation, and number of the trabeculae. Past studies that analyzed such variables after induced SCI have found general trends of reduced thickness and number, along with increased separation [47,48]. Similarly, our bone analysis results show a significantly reduced Tb.Th and Tb.N of 55% and 60%, respectively, and significantly increased Tb.Sp of 26% in injured animals compared to our normal group. Like the mechanisms discussed for the decrease in BV/TV for trabecular bone, the greater levels of trabecular bone absorption occurring compared to bone formation due to lack of viable activity from the SCI leads to the reduced trabecular number and thickness, along with an increase in the separation of trabeculae [6,8].

Passive training has been shown to significantly increase lower limb bone mass and volume, particularly in the tibia, following SCI compared to no training following SCI [8,81]. Compared to our normal group, our passively trained bike group reported its metaphyseal BV/TV to be only less than 9% of the normal group, compared to about a 16% reduction in the injury group. Trabecular number and thickness were about 79% and 80% of that of the normal group, and trabecular separation saw less than an 8% increase. Active training has also been studied and found to decrease bone degeneration, leading to increases bone volume and density, trabecular thickness and number, along with decreases in trabecular separation compared to injured animals [56—58, 81]. Our BWSTT animals saw over a 12% increase in metaphyseal BV/TV compared to injured animals, along with about a 20% increase in Tb.N and 27% increase in Tb.Th. BWSTT were over 91% of that of the normal animals for metaphyseal BV/TV.

In drawing comparisons to the results found in active and passive trained animals, it has often been found that actively trained animals had their microstructural bone values closer to that of uninjured animals than passively trained animals [8, 56—58, 81]. One such reason for this is because active training, involving the autonomy of the trainee to create some motion for themselves, generally involves active loading of the limbs [4]. This active loading and force upon the limbs, creating mechanical stresses, is thought to be one such mechanism to stimulate the formation of bone. While our BWSTT rats showed values closer to that of normal animals for trabecular thickness, number and BV/TV, it can be noted our passive bike trained rats showed values closer to that of normal rats than active BWSTT rats for trabecular separation. In human studies, more variation can be seen in bone recovery when comparing the results of passive and active training techniques [52—55].

Three-point bending in prior rat studies have found that after SCI, injury groups are unable to withstand the same load put onto the bones as normal animals [45, 48]. Bone loss that occurs following periods of inactivity and disuse can result in lower yield values, with the bones being less stiff with the loss of internal tissue [41]. Both passive and active trained animals, in connection with the lesser amounts of trabecular thickness and number lost, are able to withstand greater loads of force put upon them before failure [57,81]. Our results found that active trained bones were able to withstand an average of about 5%, or 4 lbs of force more than injury animals; passive trained animals did not experience such for load increases which may be due to the nature of the training itself—while active training relies on generating mechanical forces in rats, a possible mechanism in bone regeneration, passive training does not generally create such forces [3,4].

Muscle atrophy can be seen in inactive individuals when protein degradation overtakes protein synthesis in the muscles' tissues [25]. This trend is characterized in our results, with the injury only group having a significant decrease in soleus muscle mass to normal animals. Normal animals had a soleus mass comprising about 0.00048% of its total weight, compared to less than 0.0002% in injured animals. This is comparable to past animal studies focusing on decreases in muscle mass in the hind limbs post-SCI [43,44]. Meanwhile, trained animals saw a significantly less reduction in mass compared to injury animals. Both BWSTT and Bike groups saw their soleus mass to comprise about 0.00042% of their total body weight. Looking at the mechanisms in the body, exercising, and even stretching ones muscles initiates the synthesis of new proteins, allowing for muscle building, or mass increases, to occur [25]. All trained rats in past studies saw increases in lower limb, predominately calf, muscle mass compared to injured animals, or very slight decreases when comparing to normal animals [8, 56, 57, 81]. This study demonstrates both comparisons, such that passive training and active training had near equal results in preventing muscle atrophy in SCI rats.

5.6 Conclusion

This study provides additional results strengthening the outcome that training paradigms reduce both bone degradation and muscle atrophy, such that is seen in prior studies of similar natures [52—57]. By comparing the effects that SCI has on trained versus untrained animals, with both passive and active training methods utilized, this study also provides a comprehensive analysis on what can possibly be achieved in future studies. While the behavioral analysis tests of BBB and wire grid testing were not able to as accurately convey the final aim, the remaining bone and muscle analytic processing

and tests were successful in measuring the effects of our normal animals, along with the remaining three groups of injured, BWSTT, and Bike following a SCI from a moderate-contusion. Both active and passive training methods demonstrated the restorative effects they have on bone microstructure properties and muscle mass. The three-point bending further backed up these results. While it was unexpected that Bike animals had higher Tb.N and lower Tb.Sp values compared to active trained animals, perhaps alternative testing can give more accurate injury and testing methods, allowing for a promising future in related studies and experiments.

Chapter 6

Future Work

6.1 Introduction

There is a multitude of different training methods, as well as testing techniques, which provide alternative solutions and measures when comparing the effects that SCI has on the body. Thus far, this study has investigated the effects of SCI, specifically on the musculature and bones of the hind limbs after a thoracic level injury. Two main training paradigms, active BWSTT and passive bike training, were researched, to see how training with each of these techniques affect the bone and muscle density or area, while studying bone microstructure properties that are easily measureable in rats.

However, there exist different training paradigm methods that can be implemented in future works, to provide more conclusive and complete comparisons of which training techniques may provide more optimal results to stop degeneration, and possibly reverse it. Functional electrical stimulation (FES), briefly mentioned in Chapter 4, has become one such training method that is gaining a lot of traction in both human and animal studies, and will be discussed in more detail in the next section, along with combinational studies involving FES with either passive or active training. In addition to bone and muscle analysis of micro-CT and three-point bending, histology of the spinal cord, bone, and muscle tissue can be a useful testing technique when studying the effects injury has on the body, as well as how training can help or prevent such injuries. The results of histology for SCI will also be discussed in this chapter.

6.2 Alternative Training Methods and Paradigms

6.2.1 Functional Electrical Stimulation (FES) training. FES training is an alternative to the classic active and passive training treatments as described in Chapter 4. FES utilizes small, electrical pulse signals that are applied to, in the case of SCI patients, paralyzed muscles to help improve their functionality. Electrodes are commonly used stimulators that provide an interface for the charge to be delivered to the muscle tissue. The voltage sent from the electrode is high enough to disturb the tissues' and its neurons' resting potentials. A depolarization occurs, initiating an action potential propagating down the axon, which, in coordination, ultimately leads to muscle contraction [59]. Electrodes can be placed on the skin surface, enabling easy use by clinicians though proper placement may be difficult, or they can be implanted, which is ideal for individuals needing them for long term use [60].

Besides exercise training paradigms, FES can also be used for other assistive applications, such as breathing and grasping assistance [61]. Patients with cardiovascular conditions use FES to improve breathing function. FES exercises in one study saw oxygen uptake to be doubled, as well as ventilation rates tripled compared to those not on the training paradigm. A similar study measured a peak oxygen uptake increase of up to 103% after a year of FES training, three times a week [62]. Other advantages to FES are improved bladder function; stimulators were implanted at the sacral level to allow the injured to have improved control of their bladder and bowel movements. A known disadvantage of FES is that it can trigger autonomic dysreflexia, a condition that causes high blood pressure in individuals with higher spinal level injuries, as described in Chapter 3 [61].

In complete SCI individuals, there have been a significant number who retain some neural activity and connectivity across their injury site. In these individuals, along with those suffering from incomplete SCI, it has been shown that FES can increase electrical signals. When treated with FES in the lower limbs, increased movement along with improved ASIA motor and sensory scores, and with decreased spasticity, has been noted [62]. Stimulating the impulses of the lower extremity muscles in the proper order can also enable standing, stepping, and overall increased mobility with thoracic-level SCI persons. FES is especially best in persons suffering from T4—12 level paraplegia and still retain decent upper body strength [60].

One such process uses eight electrode channels, providing continuous stimulation to the knee, hip, and trunk extensors which enable the movement of sitting to standing to occur, along with supporting the body vertically (Fig. 38). Other FES therapies focus on keeping the patient standing for set periods of time. In this case, stimulation of hip abductors and adductors, along with the ankle plantar and dorsiflexors are included to the standard eight channels. Activation of the gluts, hamstrings, and lumbar erector spine with the aforementioned areas allowed average standing times of 10 minutes [59].



Figure 38. A patient standing with FES placed on her knee, hip, trunk extensors, and hip and trunk abductors and adductors [59]

Stepping with FES has also taken place as training. Open loop stimulation from 8 and 16 channel generators is a common delivery method, as well as stimulation from ring and walker mounted switches, or from sensors mounted directly onto the body (Fig 39). In those with incomplete SCI, step training can have a great increase in lower limb strength, walking speed and stride length. Stepping of up to 100 m can be achieved with such stimulation, with additional uses of interactive stimulation providing an extra 20% improvement in speed and distance [59].



Figure 39. A patient walking with an 8 channel stimulator [59]

6.2.2 Combination training paradigms. Many training paradigms combine the more passive bike training with FES. FES allows individuals with minimal to no lower limb movement to pedal on a stationary bike, sometimes referred to as an ergometer. While the person is biking, electrical pulses are transferred via the stimulation site. Generally electrodes are placed on the skin atop the proper muscles, allowing the person to pedal as their muscles contract and relax (Fig. 40) [61]. Patients who were trained on FES bikes 2—3 times a week for 6 months at 30 or 50 rpm saw increases in not only oxygen uptake, but also increases in muscle mass, and capillary number. Other benefits seen with FES cycling include overall improvement in muscle size, strength, fiber area and capillary area, as well as recovery of bone mass and density after degeneration [62]. Another study conducted by the Kennedy Krieger Institute's International Center for

Spinal Cord Injury combined FES with cycling training, where 25 SCI patients were matched with controls suffering similar injuries. Participants completed on average 10,000 pedal rotations a week. At the end of the over two year study, 80% of the participants saw improved motor function and 56% had improved sensory function, compared to 45% and 25% in the control group [63].



Figure 40. A patient on an ergometer, with electrodes attached to his lower limbs [64]

FES has also been combined with BWSTT in past studies. One such experiment utilized FES on the quadriceps, hamstrings, dorsiflexors and plantarflexors via an open loop stimulation on thoracic SCI patients. They were then placed onto a weight-supported treadmill with an overhead harness attached to cables and pulleys. An example of such a set-up can be seen in Fig. 41. Walking speed was determined by a physiotherapist with what was thought to be natural to the individual patient. Exercise was done 3 times a

week, for 16 weeks. Numerous tests were conducted, including having patients walk comfortably for as long as they could, up to 6 minutes, and how quickly they could walk 10 meters. Balance and spasticity were also measured, along with muscle and bone properties. No significant changes were seen in calf muscle area, though overall muscle area in the legs did improve throughout the study for the trained groups compared to the untrained, control group. While other benefits, similar to those seen in other FES trials such as coordination or motor function were better in the walking tests, it did not appear that FES combined with active BWSTT increased muscle area by a statistically relevant proportion in a short period of time [65].



Figure 41. A paraplegic walking with FES and BWSTT with leg-gait assistance [66]

Another example of combination FES training with active training includes rowing exercises. A study of 30 participants with varying SCI levels (from C4—T11) and severity (from A—D on the ASIA scale) were subjected to six months of FES rowing, with electrical stimulation present in such places including their quadriceps and hamstrings. The participants trained for 3 days/week with 20 min/session for the duration of the study. At the end, it was found that the muscles of the lower limbs were actually able to contribute towards the total aerobic capacity, demonstrating increased improvement in function that is not seen in untrained, injured persons [67].

6.3 Histology

6.3.1 Spinal cord histology. In addition to performing different training paradigms, other tests can be conducted to compare the effects of training or combinatory training versus control groups have on not just the lower limb bones and muscles, but the spinal tissue itself. Histology tests are one such option, allowing for microscopic and anatomical differences to be studied. When looking at spinal cord samples, white matter and grey matter, making up the outer and inner portions of the cord, are two important parts to study (Fig. 42). White matter contains myelinated ascending and descending nerve fibers. Grey matter contains neuron and nerve fiber cell bodies that are unmyelinated. Grey matter has been seen to begin undergoing loss within hours after severe contusion injury of the spinal cord, with the loss of white matter extending over the course of several days post-injury [68]. Looking at the amount of white and grey matter in the spinal cord is important because it is a measure of the amount of neurons and axons still viable, necessary for the performance of certain tasks. For example, the neurons in the grey matter columns are responsible for muscle movement and

recognizing stimulation, while for white matter they are responsible for being the main proponent in delivering and receiving messages in the body. Common staining techniques for viewing white and grey matter used in histology are: the H&E, or Hematoxylin and Eosin stain producing red and blue stains, and Luxol fast blue stain (LFB) to detect unmyelination and produces blue and pink stains.

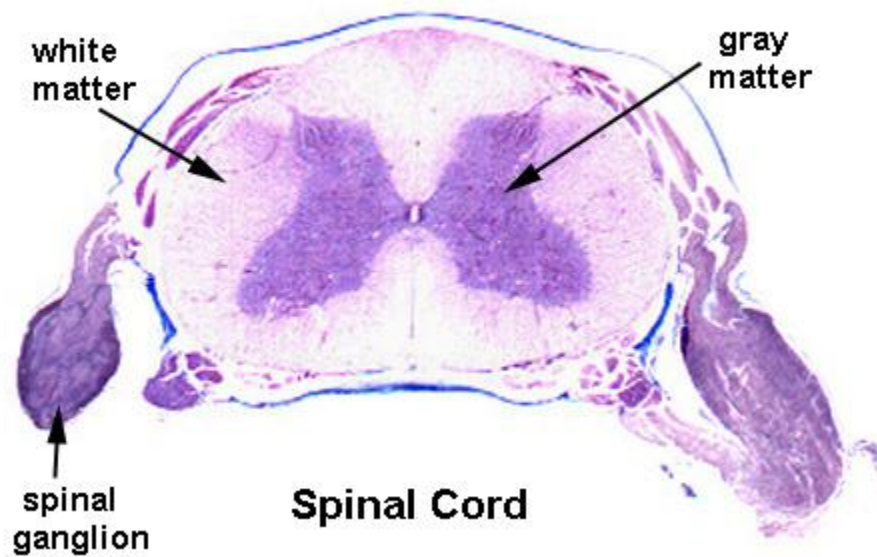


Figure 42. Histology slide of the spinal cord [69]

Studies have been conducted, mainly with animals, on looking at the changes in histology following SCI. One such study administered contusion spinal injuries via an impactor to rats at the T10 level. Animals throughout the study (from as soon as 2 hours post-injury to 10 weeks after) were sacrificed and their T10 site given histological examinations, and compared to controls. LFB staining was utilized, following

microscopic viewing (Fig. 43). When beginning the experiment, it was estimated that the average number of myelinated axons of the white matter in the dorsal column of the spinal cord was 32,200. One day after injury, the number of axons was reduced to about 8,100, and even further reduced to about 2,400 one week post-injury. A similar pattern was seen in the myelinated axons in the white matter of the ventrolateral tracts; starting myelinated axons were at around 197,600, reducing to 91,900 and 21,700 one day and one week post-injury. Cross sectional areas of both sites in the spinal column also saw decreases one week after SCI. With the use of histology, it was concluded that by 10 weeks post-SCI, the grey matter at the center of the injury site was completely gone, with small borders of white matter around the dorsal column and ventrolateral tracts. The majority of such loss was seen the first week [68].

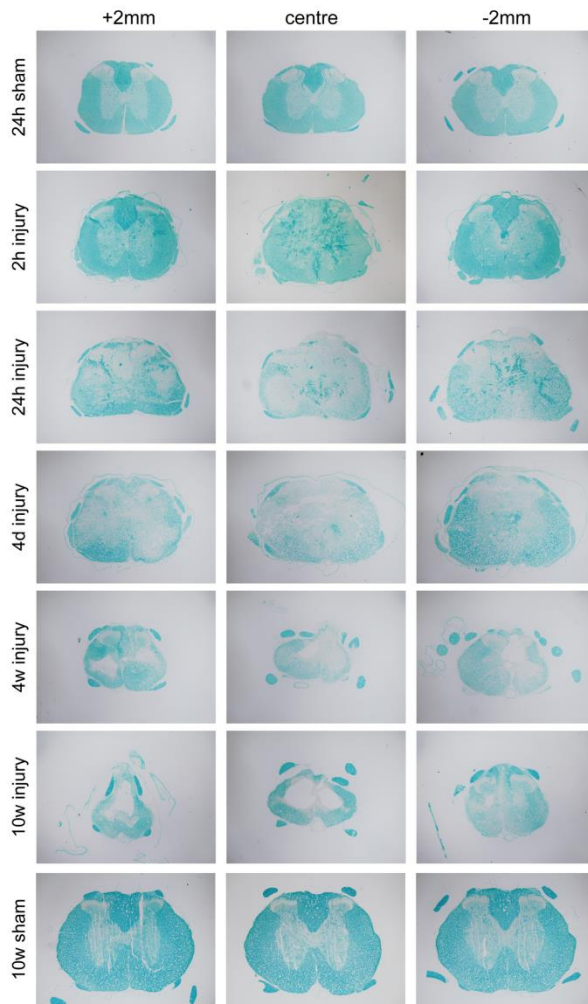


Figure 43. LFB staining of SCI and control (sham) groups comparing white matter from 24h—10weeks post injury [68]

6.3.2 Bone histology. Histology studies can also be conducted on hind bone physiology. One such study had subjects succumbed to ‘bed rest’ and inactivity for twelve weeks. At the end of the rest period, samples were taken and harvested for study. Biochemical markers of bone were noted, as well as histomorphometric analysis. Bones were prestained with Villanueva Osteochrome, dehydrated, and embedded in methylmethacrylate, before being examined under ultraviolet (UV) light. Both cortical

and trabecular bone were examined, with further toluidine blue staining carried out. Although bone mineral density was found to decrease, no significant changes in cortical bone histology was found, besides some erosion on the surface of the bone. Trabecular bone histology sample found that erosion took place, and the osteoclastic surface significantly increased from that of normal subjects. The osteoblastic surface saw a significant decline after inactivity [70].

The histology results seen in the bone were able to correlate with decreased mass and density found during analysis. Cortical bone density showed no significant decreases, whereas trabecular mass and density reduced more drastically. Trabecular thickness also showed an apparent decrease, compared to cortical thickness. Such histological analyses are therefore able to provide an additional level of confirmation to bone analysis and studying bone microstructure properties [70].

6.3.3 Muscle histology. A study on a contused spinal cord model in rats studied the loss of muscle function and mass, along with taking histology samples of hind limb muscles. Following three weeks of reduced mobilization after SCI, soleus force measurements were performed, before rats were sacrificed and muscles harvested. Comparisons were drawn people muscle weight, cross sectional area, force measurements, and fiber size from histology samples. In the soleus muscle, it was found that SCI animals had a 50% decrease in average muscle fiber size compared to normal animals. Animals that had injury in addition to immobilization casts saw a 66% reduction in muscle fiber size through histological analysis [76].

Similar to that seen in bone histology studies, conducting muscle histology studies provides more information to compare to physical analysis. In the study of muscle histology post-SCI, where injured animals were found to have reduced muscle fiber, this was able to back up other analyses. Muscle weight, for example, was found to be decreased by 20% in SCI groups, and 25% in SCI and immobilized groups. Muscle force measurements saw a similar trend, with peak force exerted by SCI rats 25% less than normals, and SCI immobilized rats 46% less than normals [76].

6.4 Conclusion

Future studies can be implemented to better expand upon what has already been experimented on in SCI literature. To get a better understanding of how the body changes and adapts following SCI, being able to study the affected areas, including the injury site of the spinal cord and column, as well as the muscles and bones of the paralyzed limbs, can give bountiful information that will better address what techniques can be applied to stop the degeneration seen in all of those areas. While new achievements are continually being made in how far one can overcome the detriments following complete and incomplete SCI, it is important to keep researching new training or combinational training techniques and looking at how they can potentially improve motor coordination and sensory function by reversing bone, muscle, and axonal loss.

References

- [1] National Spinal Cord Injury Statistical Center, Spinal Cord Injury (SCI) Facts and Figures at a Glance (2016). Retrieved March, 2017 from <https://www.nscisc.uab.edu/Public/Facts%202016.pdf>.
- [2] G. Lora, & N. McCartney, “Bone Loss and Muscle Atrophy in Spinal Cord Injury: Epidemiology, Fracture Prediction, and Rehabilitation Strategies.” *The Journal of Spinal Cord Medicine*, vol. 29(5): pp. 489-500, 2006.
- [3] J. V. Lynskey, A. Belanger, & J., Ranu. “Activity-Dependent Plasticity in Spinal Cord Injury.” *Journal of Rehabilitation Research and Development*, vol. 45(2):pp. 229-240.
- [4] G. Colombo, et al.. “Treadmill Training of Paraplegic Patients Using a Robotic Orthosis.” *Journal of Rehabilitation Research and Development*, vol. 37(6), 2000.
- [5] B. Clarke,. “Normal Bone Anatomy and Physiology.” *Clinical Journal of the American Society of Nephrology*. vol. 3(3): pp. 131-139, 2008.
- [6] B. P. McVay, et al. “Osteology (Bone Anatomy)” 2013. Retrieved March, 2017 from <http://emedicine.medscape.com/article/1948532-overview#a2>
- [7] National Cancer Institute, Structure of Bone Tissue. Retrieved March, 2017 from <https://training.seer.cancer.gov/anatomy/skeletal/tissue.html>
- [8] A. Zamarioli, et al.; “Anatomic Changes in the Macroscopic Morphology and Microarchitecture of Denervated Long Bone Tissue after Spinal Cord Injury in Rats.” *BioMed Research International*, Article ID: 853159: 9pgs, 2014.
- [9] J.T. Pramudito, et al. “Trabecular Pattern Analysis of Proximal Femur Radiographs for Osteoporosis Detection.” *Journal of Biomedical & Pharmaceutical Engineering*, vol. 1(1): pp. 45-51, 2007.
- [10] J. Chen., et al. “Age-Related Changes in Trabecular and Cortical Bone Microstructure.” *International Journal of Endocrinology*, Article ID: 213234: 9pgs, 2013.
- [11] Gray, *Anatomy of the Human Body*, Public Domain. Retrieved March, 2017.
- [12] J. Aerssens, et al. “Interspecies Differences in Bone Composition, Density, and Quality: Potential Implications for *in Vivo* Bone Research.” *Endocrinology*, vol. 139(2): pp. 663-670, 1998.

- [13] C. M. Bagi, Berryman, et al. "Comparative Bone Anatomy of Commonly Used Laboratory Animals: Implications for Drug Discovery." *Comparative Medicine*, vol. 61(1): pp. 76-85, 2011.
- [14] K.L. Moore, A.F Dalley. & M.R. Agur *Clinically Oriented Anatomy*. 1980. Retrieved March, 2017 from meded.lwwhealthlibrary.com.ezproxy.rowan.edu/book.aspx?bookid=739.
- [15] N.V. Jaumard et al. "Relevant Anatomic and Morphological Measurements of the Rat Spine." *Spine*, vol. 40(20): pp. 1084-1092, 2015.
- [16] T.M. Scalea "Does it matter how head injured patients are resuscitated?". In Valadka AB, Andrews BT. *Neurotrauma: Evidence-Based Answers To Common Questions*. Thieme. pp. 3–4. ISBN 3-13-130781-1., 2005.
- [17] W. Young. *Spinal Cord Injury Levels & Classification*. 2002-2017. Retrieved March, 2017 from <http://www.sci-info-pages.com/levels.html> .
- [18] American Spinal Injury Association & International Spinal Cord Society, International Standards for Neurological Classification of Spinal Cord Injury. Retrieved March, 2017 from http://asia-spinalinjury.org/wp-content/uploads/2016/02/International_Std_Diagram_Worksheet.pdf
- [19] Office of Communications and Public Liaison, National Institute of Neurological Disorders and Stroke. (2013). *Spinal Cord Injury: Hope Through Research*. National Institutes of Health.
- [20] M.F Newman., L.A. Fleisher &, M.P Fink. "Perioperative Medicine: Managing for Outcome." *Elsevier Health Sciences*. ISBN 1-4160-2456-5_2008.
- [21] M. Vallès, et al. "Cerebral hemorrhage due to autonomic dysreflexia in a spinal cord injury patient." *Spinal Cord*. vol. 43(12): pp. 738–40, 2005.
- [22] J.M. Piepmeyer, K.B. Lehmann &, J.G. Lane "Cardiovascular instability following acute cervical spine trauma." *Central Nervous System Trauma* vol. 2: pp. 153–159, 1985.
- [23] S. Sabharwal *Essentials of Spinal Cord Medicine*. Demos Medical Publishing. ISBN 978-1-61705-075-6. 2013.
- [24] S. Kundi, R Bicknell. &, Z. Ahmed "Spinal Cord Injury: Current Mammalian Models." *American Journal of Neuroscience*, vol. 4(1): pp. 1-12, 2013.

- [25] M Sandri, "Signaling in Muscle Atrophy and Hypertrophy." *Physiology* 23: 160-170. 2008.
- [26] A. S. Gorgey et al. "Effects of Spinal Cord Injury on Body Composition and Metabolic Profile—Part 1." *The Journal of Spinal Cord Medicine*. Vol. 37(6): pp. 693-702. 2014.
- [27] P, Vestergaard et al. "Fracture rates and risk factors for fractures in patients with spinal cord injury." *Spinal Cord*. vol. 36(11): pp. 790-6. 1998
- [28] P. Frey-Rindova, et al. "Bone Mineral Density in Upper and Lower Extremities during 12 Months After Spinal Cord Injury Measured by Peripheral Quantitative Computer Tomography." *Spinal Cord*. vol. 38(1): pp. 26-32. 2000.
- [29] S. Dudley-Javoroski &, R. K. Shields. "Muscle and Bone Plasticity after Spinal Cord Injury: Review of Adaptations to Disuse and Electrical Muscle Stimulation." *Journal of Rehabilitation Research and Development*. Vol. 45(2): pp. 283-296. 2008.
- [30] M.J. Castro, et al. "Influence of complete spinal cord injury on skeletal muscle cross-sectional area within the first 6 months of injury." *European Journal of Applied Physiology*. Vol. 80(4): pp. 373-8. 1999.
- [31] A.S. Gorgey &, G.A. Dudley. "Skeletal muscle atrophy and increased intramuscular fat after incomplete spinal cord injury". *Spinal Cord*. vol. 45(4): pp. 304-9. 2007.
- [32] C.D. Moore, et al. "Lower-Extremity Muscle Atrophy and Fat Infiltration After Chronic Spinal Cord Injury." *Journal of Musculoskeletal Neuronal Interaction*. Vol. 15(1): pp. 32-41. 2015.
- [33] Y. Dionyssiotis, et al. "Impact on Bone and Muscle Area after Spinal Cord Injury." *BoneKEy Reports*. Vol. 633. 2015.
- [34] E. Wilmet, et al. "Longitudinal study of the bone mineral content and of soft tissue composition after spinal cord section." *Paraplegia*. Vol. 33(11): pp. 674-677. 1995.
- [35] E.D. deBruin, et al. "Longitudinal changes in bone in men with spinal cord injury." *Clinical Rehabilitation*. Vol. 14(2): pp. 145-52. 2000.

- [36] C. M. Modlesky, et al. "Trabecular Bone Microarchitecture is Deteriorated in Men with Spinal Cord Injury." *Journal of Bone and Mineral Research*. Vol. 19(1): pp. 48-55. 2003.
- [37] *Trabecular Thickness (Tb.Th), Trabecular Spacing (Tb.Sp), Trabecular Number (Tb.N)*. MicroCT World. retrieved February 2017, from <http://microctworld.net/trabecular-thickness-tb-th-trabecular-spacing-tb-sp-trabecular-number-tb-n/>
- [38] M. L Bouxsein., et al. "Guidelines for Assessment of Bone Microstructure in Rodents Using Micro-Computed Tomography." *Journal of Bone and Mineral Research*. Vol. 25(7): pp. 1468-1486. 2010
- [39] M. P Gashti, et al. "Microscopic Methods to Study the Structure of Scaffolds in Bone Tissue Engineering: A Brief Review." *Microscopy Book Series, 5th Ed.;* *Formatex Research Centre*. pp.625-638. 2012.
- [40] W. Liu, et al. "Bone Micro-Architectural Analysis of Mandible and Tibia in Ovariectomised Rats." *Bone & Joint Research*. Vol. 5: pp. 253-262. 2016
- [41] M.J. Silva "Bone Mechanical Testing By Three-Point Bending." *Washington University Musculoskeletal Structure and Strength Core*. 2016.
- [42] Health and Bone, *How Does Osteoporosis Affect Bones?* Retrieved April, 2017 from http://www.healthandbone.ca/en/what_is_osteoporosis/how_does_it_affect_bones/
- [43] A. Zamarioli, et al. "Changes In Muscle-Skeletal System After Spinal Cord Injury: A Biomechanical Study in Paraplegic Rats." *Laboratory of Biomechanics—Faculty of Medicine of Ribeirão Preto*.
- [44] K. Higashino, et al, "Early Changes in Muscle Atrophy and Muscle Fiber Type Conversion After Spinal Cord Transection and Peripheral Nerve Transection in Rats." *Journal of NeuroEngineering and Rehabilitation*. Vol. 10(46). 2013.
- [45] C. C. Medalha, et al. "Temporal Modifications in Bone Following Spinal Cord Injury in Rats." *Archives of Medical Science*. Vol. 8(6): pp. 1102-1107. 2012.
- [46] M. J. Voor et al. "Bone Loss Following Spinal Cord Injury in a Rat Model." *Journal of Neurotrauma*. Vol. 29(8): pp. 1676-1682. 2012.

- [47] T. Lin, et al. "A Comprehensive Study of Long –Term Skeletal Changes After Spinal Cord Injury in Adult Rats." *Bone Research*. Vol. 3(15028). 2015.
- [48] S.D. Jiang, Jiang, Lei-Sheng &, L.Y. Dai "Changes in Bone Mass, Bone Structure, Bone Biomechanical Properties, and Bone Metabolism after Spinal Cord Injury: A 6-Month Longitudinal Study in Growing Rats." *Calcified Tissue International*. Vol. 80(3): pp. 167-175. 2007.
- [49] Fisiotek LT-P, RIMEC retrieved February, 2017 from <http://www.rimec.it/en/prodotti/fisiotek-lt-p/>
- [50] Fisiotek 3000 TS, RIMEC retrieved February 2017 from <http://www.rimec.it/en/prodotti/fisiotek-3000-ts/>
- [51] P. K Shah., et al. "Lower-Extremity Muscle Cross-Sectional Area After Incomplete Spinal Cord Injury". *Archives of Physical Medicine and Rehabilitation*. Vol. 87(6): pp. 772-778. 2004.
- [52] T. Mohr, et al. "Increased Bone Mineral Density after Prolonged Electrically Induced Cycle Training of Paralyzed Limbs in Spinal Cord Injured Man." *Calcified Tissue International*. Vol. 61(1): pp. 22-25. 1997.
- [53] A. Frotzler, et al. "High-Volume FES-Cycling Partially Reverses Bone Loss In People With Chronic Spinal Cord Injury." *Bone*. Vol. 43(1): pp. 169-176. 2008.
- [54] L.M. Giangregorio, et al. "Body Weight Supported Treadmill Training in Acute Spinal Cord Injury: Impact on Muscle and Bone". *Spinal Cord*. vol. 43: pp. 649-657. 2005.
- [55] L.M. Giangregorio, et al. "Can Body Weight Supported Treadmill Training Increase Bone Mass and Reverse Muscle Atrophy in Individuals with Chronic Incomplete Spinal Cord Injury?" *Applied Physiology, Nutrition, and Metabolism*. Vol. 31(3): pp. 283-291. 2006.
- [56] K Ertem., et al. "Effects of Different Durations of Treadmill Training Exercise On Bone Mineral Density in Growing Rats." *Biology of Sport*. Vol. 25: pp. 187-193. 2008
- [57] ,Y Joo. et al. "Effects of Endurance Exercise on Three-Dimensional Trabecular Bone Microarchitecture in Young Growing Rats." *Bone*. Vol. 33(4): pp. 485-493. 2003

- [58] Y.I. Ju, et al. "Jump Exercise During Remobilization Restores Integrity of the Trabecular Architecture After Tail Suspension in Young Rats." *Journal of Applied Physiology*. Vol. 104(6): pp. 1594-1600. 2008.
- [59] C. H. Ho, et al. "Functional Electrical Stimulation and Spinal Cord Injury." *Physical Medicine and REhabilitaton Clinics of North America*. Vol. 25(3): pp. 631-654. 2014
- [60] K.T. Ragnarsson "Functional Electrical Stimulation after Spinal Cord Injury: Current Use, Therapeutic Effects and Future Directions." *Spinal Cord*. vol. 46: pp. 255-274. 2008.
- [61] Christopher & Dana Reeve Foundation (2017). *Functional Electrical Stimulation*. Retrieved March, 2017 from <https://www.christopherreeve.org/living-with-paralysis/rehabilitation/functional-electrical-stimulation>
- [62] R. Martin et al. "Functional Electrical Stimulation in Spinal Cord Injury: From Theory to Practice". *Topics in Spinal Cord Injury Rehabilitation*. Vol. 18(1): pp. 28-33. 2012.
- [63] Kennedy Krieger Institute. "Functional Electrical Stimulation Cycling Promotes Recovery in Chronic Spinal Cord Injury". *Science Daily*. 2013.
- [64] T Schauer. & N.O. Negård "Development of Mobile and Stationary FES-Cycling Systems with Motor Assist." *Technische Universitat Berlin*. 2009.
- [65] L Giangregorio et al. "A Randomized Trial of Functional Electrical Stimulation for Walking in Incomplete Spinal Cord Injury: Effects on Body Composition". *Journal of Spinal Cord Medicine*. Vol. 35(5): pp. 351-360. 2012.
- [66] J. P McCabe et al. "Feasibility of Combining Gait Robot and Multichannel Functional Electrical Stimulation Electrodes." *Journal of Rehabilitation Research and Development*. Vol. 45(7): pp. 997-1006. 2008.
- [67] T. J. Andrew, et al. "Exercise Program for Spinal Cord Injury Based On Hybrid Functional Electrical Stimulation Row Training". *Medicine & Science in Sports & Exercise*. Vol. 47: pp. 896, 2015.
- [68] C. Ek et al. "Pathological Changes in the White Matter after Spinal Contusion Injury in the Rat". *PLoS ONE*. Vol. 7(8): doi 10.1371, 2012.
- [69] Nervous System, (2011). *Encyclopedia Science*. Retrieved March, 2017 from <https://encyclopediascience.wordpress.com/2011/05/02/nervous-system/>

- [70] J. E. Zerwekh, et al. "The Effects of Twelve Weeks of Bed Rest on Bone Histology, Biochemical Markers of Bone Turnover, and Calcium Homeostasis in Eleven Normal Subjects". *Journal of Bone and Mineral Research*. Vol. 13(10). Pp. 1594-1601. 1998.
- [71] Anatomy and Physiology, Exercise and Muscle Performance. *BC Open Textbooks*. Retrieved February 2017, from <https://opentextbc.ca/anatomyandphysiology/chapter/10-6-exercise-and-muscle-performance/>
- [72] D.M Basso., M.S. Beattie, & J.C. Bresnahan "A sensitive and reliable locomotor rating scale for open field testing in rats". *Journal of Neurotrauma* vol.12: pp. 1-21. 1995.
- [73] "Function and Classification of Bones, Classification of bones." *Anatomy & Physiology: A Learning Initiative*. 2014. Retrieved April 2017, from <http://anatomyandphysiology.com/function-and-classification-of-bones/>
- [74] JM Slade, et al. (2004). "Trabecular bone is more deteriorated in spinal cord injured versus estrogen-free postmenopausal women". *Osteoporos Int*.
- [75] CM Modlesky, S, N. Majumdar, GA Dudley. "Trabecular bone microarchitecture is deteriorated in men with spinal cord injury". *Journal of Bone Mineral Restoration*. Vol. 19: pp. 48-55. 2004.
- [76] F. Ye, et al. "Hindlimb Muscle Morphology and Function in a New Atrophy Model Combining Spinal Cord Injury and Cast Immobilization". *Journal of Neurotrauma*. Vol. 30(3): pp. 227-235. 2013.
- [77] C.H. Turner, et al. "The Elastic Properties of Trabecular and Cortical Bone Tissues are Similar: Results from Two Microscopic Measurement Techniques". *Journal of Biomechanics*. Vol. 32(4): pp. 437-441. 1999.
- [78] Paul Ducheyne, et al. "Comprehensive Biomaterials". *Elsevier Ltd*. Vol 2: Materials of Biological Origin pp. 178-179. 2011.
- [79] E. A. Zimmermann, et al. "Intrinsic Mechanical Behavior of Femoral Cortical Bone in Young, Osteoporotic and Bisphosphonate-treated Individuals in Low- and High Energy Fracture Conditions". *Scientific Reports*. 6: doi: 10.1038. 2016.

- [80] B. Busse, et al. "Increased Calcium Content and Inhomogeneity of Mineralization Render Bone Toughness in Osteoporosis: Mineralization, Morphology and Biomechanics of Human single Trabeculae". *Bone*. Vol. 45(6): pp. 1034-1043. 2009.
- [81] L.W Sun., et al "Bone and Muscle Structure and Quality Preserved by Active Versus Passive Muscle Exercise on a New Stepper Device in 21 Days Tail-Suspended Rats". *Journal of Musculoskeletal Neuronal Interactions*. Vol. 13(2): pp. 166-177. 2013.
- [82] A. P. Singh. "Cortical Bone and Cancellous Bone". *Bone Spine*. 2016. Retrieved April, 2017 from <http://boneandspine.com/cortical-bone-and-cancellous-bone/>